Reference
NBS Publi-cations

NAT'L INST. OF STAND & TECH R.I.C.
A11105 036991

NBSIR 80-1628

A11101 729005

MEASURING FEATURES OF THE FLUENCE AT THE FAR FIELD OF A CO_2 PULSED LASER--

AN ISSUE STUDY WITH SUGGESTIONS ON HOW TO DO IT

Eric G. Johnson, Jr.†
Robert J. Phelan, Jr.†

Don R. Boyle††

Electromagnetic Technology Division†

Scientific Computing Division††
National Engineering Laboratory
National Bureau of Standards
Boulder, Colorado 80303

April 1980

QC
100
.U56
80-1628
1980

QC100
.U56
no.80-1628
1980

NBSIR 80-1628

MEASURING FEATURES OF THE FLUENCE AT THE FAR FIELD OF A CO_2 PULSED LASER--

AN ISSUE STUDY WITH SUGGESTIONS ON HOW TO DO IT

Eric G. Johnson, Jr.[†]
Robert J. Phelan, Jr.[†]

Don R. Boyle[††]

Electromagnetic Technology Division[†]

Scientific Computing Division[††]
National Engineering Laboratory
National Bureau of Standards
Boulder, Colorado 80303

April 1980

U.S. DEPARTMENT OF COMMERCE, Philip M. Klutznick, Secretary

Luther H. Hodges, Jr., Deputy Secretary
Jordan J. Baruch, Assistant Secretary for Productivity, Technology, and Innovation

NATIONAL BUREAU OF STANDARDS, Ernest Ambler, Director

TABLE OF CONTENTS

		Page
INTRODUCTION		1
1.	The Free Air Breakdown Volume	2
	1.1 Purpose of this Stage	2
	1.2 Problems	2
	1.3 Potential Solutions	4
	1.4 Suggested Solution	4
	1.5 References	5
2.	A Volume Absorbing Attenuator	5
	2.1 The Purpose of the Stage	5
	2.2 The Problem	5
	2.3 The Solutions	5
	2.3.1 Accept plasma ignition	6
	2.3.2 A wedge of NaCl	6
	2.3.3 Use a mixture of SF_6 and SiF_4 injected into air flow	7
	2.3.4 Use the side lobes of the laser beam	9
	2.4 Suggested Solution	9
	2.5 References	10
3.	The Surface of the Target Board	13
	3.1 The Purpose of this Stage	13
	3.2 The Problems	13
	3.3 Possible Solutions to this Stage	19
	3.3.1 Accept the ignition of plasma	19
	3.3.2 Use a gold-plated Cu plate with holes to sample beam	19
	3.3.3 Ablation of material as a measurement tool	20
	3.3.4 A thin sheet of gold-plated copper that is super-polished	20
	3.3.5 A gold-plated copper sheet that is super-polished once	20
	3.4 Suggested Solution	21
	3.5 References	22
4.	Dealing with the Absorbed Heat to Get Beam Profile Measurements	25
	4.1 Purpose of this Stage	25
	4.2 Selecting the Necessary Thickness of the Copper Plate	25
	4.3 The Allowed Number of Laser Pulses for a Run	26
	4.4 Preparation of the Back Surface for Optimum Thermal Emission	27
	4.5 The Spatial Sampling for the Detectors	27
	4.6 Temporal Sampling of each Heat Pulse	28
	4.7 The Calorimeter Disks Cut into the Interface Plate	29
5.	Detector System	31
	5.1 Purpose	31
	5.2 Problem	31

TABLE OF CONTENTS, continued

		Page
	5.3 Solutions	31
	5.4 Suggested Solution	35
	5.5 References	36
6.	Electronics Stage	37
	6.1 Purpose	37
	6.2 Problems	37
	6.3 Suggested Solution	39
7.	Special Measurements and Controls at the Drone	40
	7.1 Purpose of this Stage	40
	7.2 The Time Pulse	41
	7.3 The Absorption Measurements	42
	7.4 Plasma Ignition Check	42
	7.5 The Heat Limit Check	43
	7.6 Orientation of the Drone in Space	43
	7.7 Air Flow Measurement	43
	7.8 Gas Flow Rates of SF_6 and SiF_4 Mixture	43
	7.9 Command Signals for Control from #1 to #20	44
	7.10 The Signal Lights	44
	7.11 Shock Gauge	44
	7.12 Sliding Door	44
8.	Software and Check List Issues	44
	8.1 The List of Needed Numerical Analysis	44
	8.2 The List of Computer Programs	45
	8.3 The Check Lists	45
9.	Calibration Issues	46
10.	Conclusions	46
	10.1 Summary of Suggested Solutions	46
	10.2 Direct Answers to the Questions Posed in Appendix A	47
11.	Acknowledgments	49
APPENDIX A		50

MEASURING FEATURES OF THE FLUENCE AT THE FAR FIELD OF A CO_2 PULSED LASER -- AN ISSUE STUDY WITH SUGGESTIONS ON HOW TO DO IT

by

Eric G. Johnson, Jr., Robert J. Phelan, Jr., and Don R. Boyle

This study examines the problems for measuring the energy density incident on targets where the energy is from a pulse of high energy at CO_2 wavelengths and where the targets are located at the far field. The analysis considers two targets--first, a ground-based target for testing and calibration of the measurement systems and second, a drone towed behind an airplane from which the energy distribution information is telemetered to the ground station. Although certain design limits are assumed, the results are general and therefore specific data about the laser sources is not supplied.

This study traces each stage of the measurement system from the reception of the incident laser pulse on the drone to the pulse-coded transmission of the sampled data to a ground-based computer.

The basic conclusion is that not all desired conditions of potential fluence can be studied. Plasma effects can prevent proper measurements. If the suggested SF_6 gas can act as a calibrated attenuator and hence avoid the plasma effects, then the range of potential fluences can be increased substantially.

Key Words: Attenuators; beam profile; calorimetry; fluence; irradiance; heat flow; measurements of temperature; plasma effects; pulsed laser beams; 10.6 μm.

INTRODUCTION

We summarize what was learned in the past three months on beam-profile measurements of pulsed laser with high fluence (J/cm^2) levels. The purpose of this study is to define a measurement scheme that can determine accurately the selected beam parameters of the fluence when the laser pulse is at the far field and when the site for this far field is either a drone flying at distances of 1 or 3 kilometers from the laser or is a fixed site 600 meters from the laser. (Appendix A shows the work statement. The questions posed in this statement are answered in the conclusion of this report.)

Design of a properly operating measurement system can be very complex when the conditions have large and variable dynamic range. To establish a rational process for selection of the "best" design we subdivide the measurement system into a series of stages each of which are discussed in an individual section. Within these sections we address the purpose of the stage, what are the problems and solutions to those problems. Each solution has listed its advantages and disadvantages. Finally, each section has a specific recommendation for a solution to this stage under either the conditions of the drone or of the fixed site

environments. In some cases there is information missing which is necessary for a best decision. We then define a procedure to learn the necessary information.

These sections are organized according to the sequence in which the information about the fluence distribution would be processed, namely starting from reception of the incident laser pulse through the detector unit and finally a pulsed-coded signal from the transmitter to the ground based computer-receiver unit. In each section, the basic concepts are defined and a solution is shown subject to key issues and their appropriate answers. Many design details, such as machining, placement of screws, size of parts and actual experimental design, are not given in this report. Many decisions and tests are necessary to select those details.

The selection of a solution within each stage is decided by what will preserve the information about the fluence to the desired accuracy and by what will permit some useful measurements if there is a failure in the assumptions. This design strategy is critical at the surface of the target board* where the conversion of laser energy to heat takes place. It is possible that the target board will cause plasma ignition and hence there will be no way to measure properly the beam profile without the convolution effects of the plasma.

Each section has its self-contained references, tables, and charts. This allows the reader to identify sources for each stage without confusion from other stages.

Finally, the conclusion contains an overview of the situation with a brief summary of the suggested solution along with answers to the questions posed in the work statement.

1. The Free Air Breakdown Volume

1.1 Purpose of this Stage

We are concerned with a parallelepiped with a 23 cm cm by 60 cm cross-section area in front of the target board and a height corresponding to the region of potential air breakdown when the laser pulse comes within this volume. This stage corresponds to the region for potential plasma ignition without the influence of the target board. There are limits in the irradiance (W/cm^2) and the fluence (J/cm^2) which will pass through this volume without plasma ignition. We identify those limits and give estimates of the size of this volume. (The limit of 23 cm x 60 cm is determined by the area on the drone available for beam diagnostics.)

1.2 Problems

The attached Figure 1.1 shows the air breakdown conditions for laser radiation [1]. From this graph we find several limits to the irradiance (intensity) allowed for propagation without air breakdown to the target board. The two limits to irradiance arise because the expected laser pulse has two parts; namely, a gain-switched spike and the main pulse. The gain-switched spike has about a 0.3 μs pulse length and an average peak irradiance that is expected to be four to five times the average peak irradiance of the main pulse. This main pulse has a length of about 10 μs. (We will assume in this report that the pulse shape is

---

* This is the label for the unit that will perform the measurements of fluence.

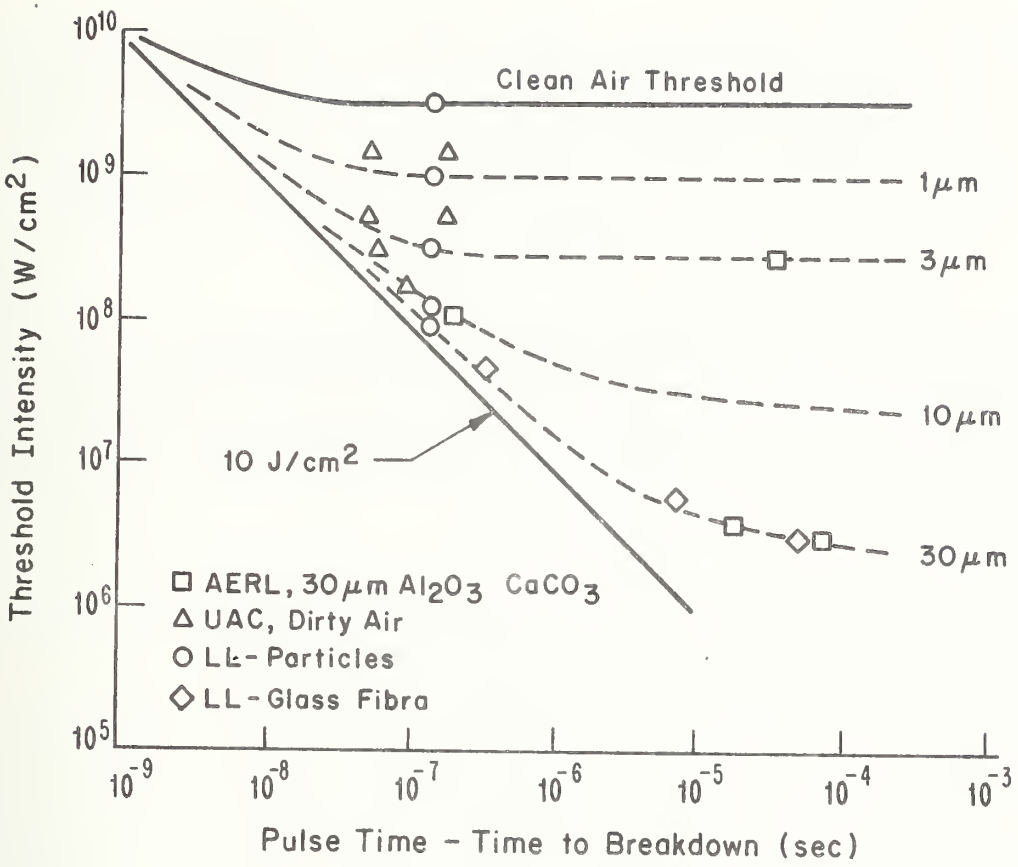

Figure 1.1 Measurements of Air Breakdown in the Presence of Particulate Matter (Reproduced from Ref. 1). The micrometer parameters on the right are the diameter of the dust particles. The threshold intensity is required to produce a plasma. For example, an intensity (flux) of 100 MW/cm^2 will ignite a plasma if the pulse lasts at least 0.1 μs.

two rectangular pulses with the gain spike being five times the main pulse (5 I_0) and leading it. This spike has length of 0.3 μs. The main pulse will have an irradiance of I_0 and a pulse length of t_0 = 10 μs. The fluence of the spike is 1.5 I_0 (J/cm^2), and the total fluence is 11.5 I_0 (J/cm^2) where I_0 is in MW/cm^2 units.)

Using the 10 J/cm^2 limit for the spike, the gain spike limit requires that the $I_0 \leq 6.7$ MW/cm^2. The figure 1.1 for 30 μm particles implies the main pulse limit requires that $I_0 \leq 5$ MW/cm^2. Because the process of plasma ignition is statistical and because the particle size is not necessarily the 30 μm particles, we assume that I_0 could reach 10 MW/cm^2 at the target board. Using this value we have some safety in design for the heat load and damage estimates on the target board.

This potential for air breakdown and possible heating of the dust particles in this volume means that this volume must be cleared between each pulse. For the sites using the

drone, its motion of about 150 m/s will clear the volume. For the fixed site, we will need to put fans to clear this volume. A wind of 1 m/s will allow a maximum pulse rate of 1.7 per second. A wind of 10 m/s will allow a maximum pulse rate of 17 per second, and a wind of 100 m/s will allow a maximum pulse rate of 170 per second.

The depth of this volume along the optical axis is given approximately by this formula

$$I_m/(1+(\lambda h/\pi w_0^2)^2) \leq 5 \text{ MW/cm}^2 \quad , \tag{1.1}$$

where I_m is the potential peak irradiance (ignoring air breakdown and beam quality) at the focal plane of the target, h is the minimum height of the volume in front of the target, w_o is the radius of the spot size of the beam at the target, and λ is wavelength, namely 10.6 μm. The table 1.1 shows examples of possible values for h given I_m and w_o.

Table 1.1. Examples of height for the parallelepiped region of potential air breakdown. Values are approximate.

I_m(MW/cm^2)	w_o(mm)	h(m)
10	30	30
10	30	300
5.5	10	9
5.5	30	90

1.3 Potential Solutions

It is necessary to deliver the energy without air breakdown because its occurrence causes substantial attenuation of the laser radiation delivered to the target board.

To avoid free air breakdown it appears to be necessary to keep the I_m below the 5 MW/cm^2. In this case, the height, h, will be zero and this stage can then be ignored. Reference 2 suggests it may not be necessary to keep I_m below 5 MW/cm^2. If this proves to be true, then the limits for I_m shift to the target board.

1.4 Suggested Solution

Ignore the implications of reference 2, it is an unlikely situation. Keep the I_m below the 5 MW/cm^2 during a measurement sequence. We assume that this can be done for the desired measurements in this report. If air breakdown does occur, the delivered fluence to the target board will be substantially less than the potential 58 J/cm^2 implied by this limit. This situation implies no problems to the target board and thus will be ignored except there needs to be detectors to record when air breakdown occurs. We suggest that output from the target board as well from the optics steering system at the laser can be used to verify free air breakdown. These detectors can be placed so that they see a side lobe of the laser beam.

(See Section 7.) They will also be used to provide timing information.

Keeping this I_m less than 5 MW/cm^2 may require defocusing of the beam with the consequence that it is no longer a far-field pattern. This implies substantial changes in the measured pattern. A better method would be to use a lower energy laser beam from the source. A large NaCl beam splitter or a weak attenuator of SF_6 in the near field may be needed to get the required level of attenuation.

1.5 References

[1] D. E. Lencioni, Presentation at HELREG Subpanel Propagation Meeting, November 18, 1975, MITRE Corporation, Bedford, Mass.

[2] D. E. Lencioni and J. E. Lowder, Aerosal Clearing with a 10.6 μm Precursor Pulse, IEEE Journal of Quantum Electronic, Vol. QE-10 #2, Feb. 1974, page 235.

2. A Volume Absorbing Attenuator

2.1 The Purpose of this Stage

Even if the peak irradiance is kept less than the 5 MW/cm^2, it is possible for a plasma to be ignited when a laser pulse strikes the surface of a solid [1]. This section explores the possibility of attenuating the laser beam with a volume absorber of gas so that the irradiance striking the solid will not cause plasma ignition. Reference 1 concludes that prompt ignition for the pulse shape defined already can occur at I_o = 0.2 MW/cm^2 from the gain spike and I_o = 1 MW/cm^2 from the main pulse. To maintain the plasma, we require the latter value for I_o.

2.2 The Problem

We wish to make measurements of the fluence distribution. When a plasma is ignited, it causes the fluence distribution to be changed in time and space. The net result is a distortion on the special and temporal form of the heat deposited on a solid material. The distortions are due to the fact that: (1) the time rate of decay by recombination of the plasma is near 0.1 ms and (2) the spatial spreading of the energy is near one to three centimeters. The former fact means that details of pulse shape less than 0.1 ms will be washed out if plasma ignition occurs. Since we are only interested in the fluence, this situation has no serious consequences. Because the air is flowing at 50 m/s around the drone and because of the way the plasma develops, we get shifts in position of the fluence center of about 1.5 cm and spreading of the radius of the beam of about 3 cm. At the fixed site the shift in position will be less than 1 cm. This spatial spreading will wash out the position and value of the peak fluence.

2.3 The Solutions

Given the above conditions, we want to avoid ignition of plasma. We have three methods available to avoid this ignition. First, we attenuate the laser beam with a volume attenuator or with a wedged beam splitter. Second, we fix the surface and type of solid used for

measurements so that the threshold of ignition is raised above the 0.2 MW/cm^2. Third, we reduce even further the allowed peak irradiance from the laser. We try to use features of the first two methods because we do not want to avoid these levels of irradiances at the target borad. As a fall-back position, we accept that one solution is to allow plasma ignition with all its defects.

2.3.1 Accept plasma ignition

In this case, we decide that the real goal of this measurement program is not to measure the distribution of the incident laser beam, but is rather to measure the distribution of the absorbed heat in the target board whether or not the plasma is present. This solution avoids the need to concern ourselves with the details of the beam propagation, plasma ignition, and deposition process. Rather we accept a particular target for measurement under the field conditions and use it as a baseline reference on what to expect for other potential targets under these same field conditions. The disadvantages of this solution come because we may have peculiar features such as the nonlinearity of absorption of a given target board distorting our decisions on how the laser system acts on various targets. Also this technique limits greatly the ability to predict what will happen under new field conditions since we would have eliminated our check of the theoretical models.

Current laser effects studies have tended to settle for this method. Their measurements do not show the pulse to pulse details of the fluence pattern at the target [2,3,4]. There is current debate about what is the actual beam pattern in their tests.

2.3.2 A wedge of NaCl

Current data [5] on the peak fluence handling capabilities of a large 30 cm diameter wedge of NaCl are 4 J/cm^2 at the single pulse rate with 1 ns length. The opinion of persons in the pulsed laser field [6] are that NaCl, KCl, and ZnSe all should take the design level, 120 J/cm^2, easily for the 10 μs length pulses of the type under consideration. ZnSe appears to have higher risk for this level [7,8]. There is no information of what is the allowed pulse rate. Suggestions are that the limit [7] is due to single pulse catastrophic damage and not the pulse rate. Obviously, too high of a pulse rate must cause eventual problems. Since this design threshold is above the air breakdown limit, a wedge is a viable technique for getting information about the beam profile at the fixed site if water vapor is eliminated as a problem [9]. The first reflected beam in an NaCl wedge for an incident beam at 120 J/cm^2 would be at 5 J/cm^2 level. This beam should have no plasma breakdown problems for a stainless steel diffusing plate. (Page 27 of reference 2 suggests a design limit of 4 J/cm^2 for an unpolished anodized Al plate.) The second transmitted beam from the wedge will be 0.2 J/cm^2 level. This beam could be absorbed by a teflon sheet on a metal substrate (a cooking pot) without damage and would show a rise of tens of degrees Centrigrade. (See page 26 of ref. 2.) Both beams can be scanned with a TV type system provided the scan rate can be synchronized to the pulse rate of the laser so that the measured output can look at the pattern on a pulse-to-pulse basis.

The advantages of this wedge sampling technique is that the beam sample is a linear sample of the incident laser beam after the propagation through the air and that the resulting sample can be studied by many beam profiling techniques [2,10-14] including TV scan systems [2,15,16].

The disadvantages of this technique are that there is insufficient space on the drone for such a method and that there is some chance for these wedges to be affected adversely by the environmental conditions at the fixed site. It will be necessary to do some form of environmental control around the wedge to prevent a significant lowering of the damage threshold. If an NaCl wedge can be obtained for the fixed site that can be verified to take the 120 J/cm^2 level, then it should be used. Measurements with large spot size beams suggest NaCl can do the job [17,18,19]. One very important disadvantage could come from an accidental plasma ignition at the wedge. This would cause damage by extreme heating of the surface of this wedge. Thus it is necessary to avoid air breakdown in the neighborhood of this wedge. This can be done by being very sure that the air breakdown point of the laser beam is after the wedge by at least 10 meters. Test shots without the wedge could identify these conditions. This implies the need for techniques to detect the air breakdown plasma. We suggest that looking at scattering of the laser beam with the ir scanning equipment will be the best technique since a low electron density plasma does not always radiate significant visible light. It is most likely that a plasma ignition will have significant visible light.

2.3.3 Use a mixture of SF_6 and SiF_4 injected into air flow

The two previous solutions have unacceptable features for use in the drone. The acceptance of plasma ignition is retreat from direct beam profile measurements and the wedge cannot fit on the drone; therefore we look at a moderate risk idea, namely we see if a gas, which is a strong absorber of 10.6 μm, can be mixed in the turbulent air within the boundary layer just in front of the target board. Here we assume this board is on the side of the drone. A flat plate [20,21] system will show a boundary layer of turbulent air with a thickness of

$$y = 0.37 \times \left(\frac{ux}{v} \right)^{-0.2} ,$$

where x is the distance from the start of the turbulence, u is the velocity of gas flow parallel and across the plate, and v is the kinematic viscosity of the gas. For example, if $x = 1$ m, $u = 100$ m/s, and $v = 1.8 \times 10^{-5}$ m^2/s, then $y = 1.7$ cm. For these flow conditions the stability of this thickness, in a statistical sense, is better than 1 percent. (See pages 24-25 of reference 21.)

Given the above situation, we could inject some known mixture of SF_6 and SiF_4 at a known rate to cause a known attenuation of the incident laser so that the peak irradiance is below conditions for plasma ignition on the surface of the target board. A practical level of attenuation is one order of magnitude. Thus, we can reduce the design level from 120 J/cm^2

to 12 J/cm^2. This implies an I_o = 1 MW/cm^2. Given the results of reference 1, this gets the beam irradiance to the level where it may be possible to prevent prompt plasma ignition. This issue will be discussed in the next section.

The gas SF_6 has an absorption [22] of about 90 percent for the 2 cm boundary layer thickness when SF_6 is 1 percent of the volume of gases in this layer. This SF_6 can be injected into the boundary layer along a line before the target board. To get good mixing it is estimated to take at least 30 cm before the target board. (A test will have to be made.) References 24 to 29 cover key technical features of SF_6.

The prime question remaining is how well the absorption of the gas can be measured when the drone is in flight. What is a possible strategy? There are at least four elements in the strategy:

1. First, make a series of runs with the laser system and drone without the SF_6 and keep the irradiance below plasma ignition for the target board. Second, repeat these runs under the same conditions, namely same speed of drone, same atmospheric conditions, same optical conditions, but with SF_6 and with increased gain of the electronics for the target board. Finally, use the results of calibration for the response of the target board to the laser beams to infer the spatial absorption structure of the SF_6. (See section 7.)
2. Mount some form of pulsed laser and optics on the drone so that selected segments of the SF_6 gas can be directly illuminated for a real time absorption measurement. Have a line of detectors on the up-wind and a second line of detectors on the down-wind side to observe the absorption of the SF_6. To complete the calibration, this same setup would make measurements when no SF_6 was in the flow stream. This setup will be difficult, if not impossible.
3. Because there is a strong chance of nonlinearity or a spatial convolution due to the rapid heating of the air in the boundary layer, it is necessary to test what are the effects of this gas expansion. By varying the mixture of gases using SF_6 and SiF_4 in the injected gas, we can control the level of absorption of 10.6 μm radiation.

   The gas, SiF_4, has no significant absorption at 10.6 μm [30]. Unlike SF_6, it is considered toxic [31] and therefore will have to be handled with care. If only a small percentage of this gas is used, this problem should be minimum. This SiF_4 is selected because it has an atomic weight and viscosity comparable to the SF_6 and thus should minimize the change in flow due to injection of the SF_6-SiF_4 mixture.

   If the controls for injection of SF_6 are good enough and the process of injection does not significantly disturb the boundary layer, then it will be better and easier to just vary the percent of SF_6 in that layer by reducing or increasing the injection rate of SF_6.
4. If this attenuation process proves to be reliable, it may be possible to image the beam profile by observing the reradiated energy in the SF_6 flow with a far infrared camera operating at appropriate scanning rates or with a two-dimensional array. This approach should be tested at the fixed site. The reradiated energy should be observed from behind and in front of the SF_6 stream.

There is expected no visible radiation. If it occurs, then plasma ignition has probably occurred. From the preceeding, it is complex to determine the absorption profile of the SF_6. It would be much nicer to forget the whole thing. Unfortunately, the alternative is to allow plasma ignition and all the problems implied by it. Therefore, some testing at the fixed site of the SF_6 concept seems worthwhile.

The advantage of this technique is that we can measure all of the desired beam parameters. The disadvantage is that the peak fluence may not be as accurately determined as desired if we are unable to get a good measurement of the absorption. A further disadvantage arises from the reradiated energy. It can cause some error in the measured fluence deposited on the target board. Current data suggests this is unimportant here [28].

2.3.4 Use the side lobes of the laser beam

If the above solutions fail or if there is need for a secondary check, then it could prove useful to measure the side-lobe pattern. This method has the advantage that there is little chance for the plasma effects and for the propagation process to change the pattern of these side lobes once the far-field pattern has been developed. It is possible to infer a center of the main beam neglecting its distortion by the nonlinearities in the propagation process. A disadvantage of this solution is that it will not be possible to infer what is the true peak fluence or what are the beam profile details of the main beam. Nevertheless, details about the jitter from pulse to pulse could be inferred from side-lobe measurements. This information can be used simultaneously with the measured results of deposited heat during plasma ignition of the main lobe to generate the relevant parameters for the evaluation of the laser system.

2.4 Suggested Solution

The above discussion shows that there is no certainty in the path for a proper beam profile measurement. It is necessary to keep open the options and to accept that no scheme will work. Therefore, we suggest the solution for this stage is:

1. Assume the plasma ignition will occur and design the target board so it can take the ignition with minimum cost of repair.
2. Try to avoid ignition by using the SF_6 and test if the absorption process can be made accurate enough for the desired beam profile measurements.
3. Get three NaCl wedges of 8 cm diameter made using the same processes as the 30 cm wedge to verify what is the level of fluence this manufacturing process can take and what is the allowed rep rate. Specify a maximum surface absorption (and scattering) level to eliminate problems with polishing materials and to specify smoothness. Use these results to control the allowed use of the 30 cm wedge at the fixed site. If it can take the full design range of 120 J/cm^2 and the full rep rate, then the calibration process at this site will be greatly simplified and the testing program will have minimum extrapolation. If the 30 cm wedge cannot take the desired design specifications, then the testing program will have to be modified with the addition of less direct measurement techniques such as looking at the scattered pattern off the plasma

or off the SF_6 flow under the conditions that the fluence level is above the limits of the wedge. This system for scattering measurements should be calibrated with the wedge under the conditions it can be used. In this case, a diffused scatter of either anodized Al or stainless steel #304 can be used in the secondary beams. Simultaneous with the measurements of the scattered radiation will be the measurements from the target board system and from the reference system to calibrate it.

4. Calibrate all systems at the fixed site over the ranges where they can operate and use those results to reduce the uncertainties of the drone system when it is used under conditions not accessible to direct calibration.
5. Accept that there will need to be extensive calibration corrections to be stored and used in a ground-based mini-computer system at the fixed site.
6. Fans are needed to move the air at the fixed site and to cause a flow of an air-SF_6 mixture so absorption measurements can be done at this same site and so debris and effects of the previous pulse are removed. We expect the maximum speed of flow to be around 20 m/s. These are large fans used in movies. Thus this flow will not duplicate the conditions of flight for the drone which is expected to be near 150 m/s. These activities imply air flow measurements in the drone and at other points in the fixed site.
7. Consider all the suggested methods for absorption measurements and implement as many as possible. There should be at least three detectors in the up and down stream points on the drone so that we can get real time measurements of absorption. (See section 7.) With this number of detectors, distortions in the gas flow may be evident.
8. Borrow wherever possible equipment that has already been developed for laser pulse measurements such as that at AFWL, MIRADCOM, NRL, and various commercial firms. Equipment with a measurement history has great value in calibration procedures. The equipment of highest utility are those unique ir detection systems.
9. The suggestion of workers in the field is that it is necessary for the experimenters to do their own etching and polishing of the wedges of NaCl or KCl. If that proves necessary, then three references can be of value [32,33,34]. The techniques given in reference 34 may be a way to avoid the polishing process and yet get high damage thresholds. Unfortunately, it has not been tested on the last point.

2.5 References

[1] A. A. Boni, F. Y. Su, P. D. Thomas, and H. M. Musal, Theoretical Study of Laser-Target Interactions--Final Technical Report #SAI 77-567LJ. See pages 2-6 and 2-7 for key formulae. (a) Vapor breakdown is $F \geq 1$ J/cm^2 fluence, and $I \geq 0.4$ MW/cm^2 irradiance during the fluence deposition at one atmosphere pressure and at 10.6 μm wavelength. (b) Prompt breakdown is $F \geq 1$ J/cm^2 fluence with the irradiance satisfying both $I \geq 1$ MW/cm^2 for air breakdown and $I \geq \frac{0.25 \text{ MW/cm}^2}{\alpha \cos \theta}$ for induced vapor or electron seeding by the surface of solid target. Here α is absorption and θ is angle of beam relative to the normal of surface.

[2] C. T. Walters and R. E. Beverly, III, Final Report on Diagnostic Coordination Task, Battelle Report of October 7, 1977 to the U.S. Army Scientific Services Program. This report is an important summary of current diagnostics for pulsed laser beams at 10.6 μm and at 10 μs pulse length.

[3] R. W. Mitchell, E. L. Roy, R. W. Conrad, Handbook of Laser Effects and Vulnerability--AD-C010335. An important classified compilation of past measurements and theory.

[4] Private communications with: R. W. Conrad, MIRADCOM; R. Rudder, AFWL; J. T. Schriempf, NRL; R. Stegman, NRL; S. Lyons, AFML; J. Woodroffe, AVCO; R. Wenzel, NRL; C. Walters, Battelle.

[5] Private communications with J. Sollid, LASL, and D. Cope, Harshaw Chemical.

[6] Private communications with J. Smith, AVCO.

[7] H. E. Bennett, Thermal Distortion Thresholds for Optical Train Handling of High Pulse Powers, page 11, Laser Induced Damage in Optical Materials (1976), NBS Special Publication 462.

[8] R. Gibbs and R. M. Wood, Laser-Induced Damage of Mirrors and Window Materials at 10.6 μm, page 181, Laser Induced Damage in Optical Materials (1976), NBS Special Publication 462.

--See also other papers in the publication for issues of damage threshold.

--S. Sharma, R. M. Wood, and R. C. C. Ward, Measurement of Mirror and Window Characteristics for Use with 10.6 μm Lasers, page 183, Laser Induced Damage in Optical Materials (1977).

[9] V. I. Kovalev, F. S. Faizullov, Investigation of Surface Breakdown Mechanism in IR-Optical Materials, page 318, Laser Induced Damage in Optical Materials (1978) NBS Special Publication 541.

[10] R. J. Licata, Beam Profiling of a Multimode Laser, AD-A064314.

[11] L. A. Young, J. A. Woodroffe, E. R. Bressel, Laser Effects Assessment Program, AD-B026974L.

[12] S. Marcus, J. F. Lowder, S. K. Manlief, Laser Heating of Metallic Surfaces, AD-A028580.

[13] R. V. Wick, A. C. Saxman, and E. A. Blankenship, Real Time Intensity Profiling and Beam Divergence Measurements of a Laser Beam, page 294, Proceeding of Electro-Optical System Design Conference (1973).

[14] B. Contreras, The Current Target Board System on a Drone at AFWL. Here we have a cw irradiance limit near 20 kW/cm^2 for damage to thin film detectors, so we may need a further reduction of peak beam irradiance by 50 times to use this setup without modification.

[15] J. T. Klopcic, J. E. Kammerer, Procedure for the Reduction of IR Scanner Data, AD-A039919.

[16] J. Thomas, D. Norrie, and J. Holtz (Lockheed) JANAF Repetitively Pulsed Vulnerability Effects, LSMC-D012989 and LSMC-D563648. Here an ir scanning system was used to look at the beam profile for repeated pulsed laser beams at 10.6 μm.

[17] J. L. Stanford, R. W. Pierce, K. E. Camblidge, C. N. Helmick, and W. P. Norris, ARPA Laser Window Technology Validation Program, page 30, Proceeding of the High Power Laser

Optical Components and Components Material Meeting (1977). This is one of a series of reports for a continuing program. Once the design details for the fixed site have been settled, we suggest a communication with J. L. Stanford to establish the manufacturer and the material to be used as a wedge which will not fail at the 120 J/cm^2 design level. Present indications are that NACl will work. (Surface absorption is the issue.)

[18] A manufacturer indicates an estimated cost of $5000 for using polycrystal NaCl and $2500 for single crystal NaCl of a single 30 cm diameter wedge of 5° and with a scratch/dig of 40/20. The optical figure of $\lambda/10$ is more than adequate. The 5° wedge will allow separation of a 30 cm diameter beam in about 4 meters.

[19] Here we include a number of references for background:
--Compendium of High Power Infrared Laser Window Materials AD-901886.
--Review of Gas-Breakdown Phenomena Induced by High-Power Laser-I, RCA Review, vol. 35 (1974) page 48.
--Beam Diagnostics for High Energy Pulsed CO_2 Lasers, Applied Optics, vol. 13 #2, (1974), page 314.
--Transmissive Optics for High Power CO_2 Lasers: Practical Considerations, Optical Engineering, vol. 17 #3, page 225.

[20] Private communication with Gene Stewart, NBS.

[21] L. D. Lorah, Aerodynamic Influences on Infrared System Design, pp. 24-22 to 24-29, The Infrared Handbook, Library of Congress Catalog Number 77-90786.

[22] A. V. Nowak and J. L. Lyman, The Temperature-Dependent Absorption Spectrum of the ν_3 band of SF_6 at 10.6 μm, page 945, J. Quant. Spectrosc. Radiat. Transfer, vol. 15 (1975). Here the absorption coefficient $\alpha = 218\ cm^{-1}$ for standard atmosphere of SF_6 and $\alpha = 0.218\ cm^{-1}$ for 0.76 Torr.

[23] Sol Aisenburg, A Study of the Use of Chemical Additives for the Alleviation of the Plasma Sheath Problem, AD-829211.

[24] J. D. Anderson, CO_2 Laser Radiation Absorption in SF_6-Air Boundary Layers, AD-751016. Here are wind tunnel measurements using cw laser with SF_6 as an absorber of the radiation.

[25] J. D. Anderson, A Numerical Analysis of CO_2 Laser Radiation Absorption in SF_6, AD-768752. Companion paper to reference 24.

[26] W. H. Reichelt, E. E. Stark, Jr., T. F. Stratton, A Gas Calorimeter for Use at 10.6 μm, page 305, Optics Communications, vol. 11, No. 3 (1974). Here SF_6 is used for conversion of 10.6 μm radiation into an integrated pressure change.

[27] V. S. Letokhov, Laser Selective Photophysics and Photochemistry, page 33, Progress in Optics, vol. 16, (1978), North-Holland Publishing Company, L. C. No. 61-19297. Here we find the multiple photon dissociation threshold for pure SF_6 is 20 MW/cm^2 for pressure of 0.2 Torr and for 90 ns pulses. Below this irradiance level dissociation is insignificant.

[28] R. D. Bates, Jr., J. T. Knudtson, and G. W. Flynn, Laser Induced Infrared Flourescence: Thermal Heating, Mass Diffusion, and Collisional Relaxation in SF_6, page 4.74, Journal of Chemical Physics, vol. 57, No. 10 (1972).

[29] Handbook of Matheson Gas Products, page 521. Describes properties of SF_6. It is considered non-toxic.

[30] E. A. Jones, J. S. Kirby-Smith, P. J. H. Woltz, and A. H. Nielson, The Infrared and Raman Spectra of SiF_4, page 242, Journal of Chemical Physics, vol. 19, No. 2 (1951).

[31] See page 509 of reference 29 for properties of SiF_4. This gas is considered toxic.

[32] M. J. Soileau, H. E. Bennett, J. M. Bethke, and J. Shaffer, Polishing Studies and Backscatter Measurements on Alkali-Halide Windows, page 20, Laser Induced Damage in Optical Material: 1975 NBS Special Publication 435. Here we find that polishing can increase surface absorption.

[33] H. Vora, M. C. Ohmer and T. G. Stoebe, A Comparison of Bulk and Surface Absorption in NaCl and KCl between 9.2 and 10.8 μm, page 24, Laser Induced Damage in Optical Materials (1978). Here we get data on the latest absorption coefficient for polycrystal materials. This data gives an indication of the state of the art.

[34] R. H. Anderson, J. M. Bennett, Optical Properties of KCl Forged Between Optically Polished Dies, page 65, same publication as reference 33.

3. The Surface of the Target Board

3.1 The Purpose of this Stage

This stage has two purposes, namely first to absorb a known portion of the incident fluence with a known dependence on the fluence and second to deflect and defocus the unabsorbed fluence away from the target board and toward the ground or to some other energy dump. The first purpose has significant problems and is addressed in this section. The second purpose has no quantitative features, therefore, it is easily satisfied by doing the following. The plate used to intersect the laser beam will be polished and will have a diverging radius of curvature of 10 meters or less to defocus adequately the reflected laser beam, and the plate will be mounted so that the optical axis has a 5-degree change toward the ground or toward the energy dump. At the fixed site the reflected laser beam will have to be carefully considered because there can be the ir scanners, the wedge of NaCl, and other equipment in the path of this beam. Damage or measurement errors could result. The front of the energy dump could be a highly polished reflecting sheet of cold-rolled copper (that may be damaged and/or ignite plasma) set to deflect the reflected beam by 90 degrees into absorbing material such as carbon, plexiglass, anodized Al, and dirt. This absorbing material should be at least 10 meters away from the measurement systems and should produce diffuse reflections. It may prove necessary to use plexiglass to isolate the energy dump from measuring equipment. The reflection off the ignited plasma on the copper sheet will also have to be considered.

3.2 The Problems

For our discussion of this stage, we assume that the peak irradiance can range from 0.1 to 10 MW/cm^2 or a fluence of 1 to 120 J/cm^2 depending on the conditions of the incident laser beam and the site used to make measurements.

There are three possible situations for laser beam interaction at this interface. First, there is no plasma ignition. Second, there is prompt or local plasma ignition. Third, there is general plasma ignition. For accurate measurements of the laser beam profile, we want to avoid any plasma ignition. Once it occurs, there can be damage to the target board and we lose any chance for accurate measurements because of the convolution effects of the plasma and the changes in the absorption coefficient of the target board. This situation is shown by the references 1-22 in this section. The following paragraphs extract the key issues from the literature as we try to find a way to avoid plasma ignition [23-44] in our quest for meaningful beam profile measurements.

The local plasma ignition due to flakes of metal or oxide is the most difficult problem to solve and may have no solution for the design parameters. Before we attempt a solution, we must identify what can be done to avoid the bulk plasma ignition process and then work from these conditions to raise the threshold of fluence for the local plasma ignition process as high as possible.

The bulk plasma ignition is avoided by using materials for the target board that will not melt under the conditions of the applied laser pulses assuming no plasma is ignited by the local plasma ignition process. Table 3.1 summarizes thermal and absorption properties

Table 3.1. Selected materials that may be used in the beam sampling plate.

Material	Conductivity K (J/(cm·s· K))	Specific Heat Cp(J/gm· K)	Density ρ(g/cm^3)	Melting Temperature T_m(°C)	Absorption Coefficient α (polished)
Al	2.27	0.95	2.70	657.1	0.02
Cu	3.89	0.384	8.94	1080	0.015
Mo	1.45	0.271	10.2	2620	0.02
Au	9.96	0.128	19.3	1063	0.02
Stainless Steel	0.16	0.50	8.02	1420	0.1
Aluminum Oxide	0.346	0.728	3.5	2050	0.98
Cu O	0.175	0.125	6.4	1026	estimate 0.7
Graphite	1.3	0.741	1.86	3652	0.9
Ni	0.56	0.460	8.91	1449	estimate 0.5
Be	1.59	1.88	1.85	1278	0.5

of selected materials that could satisfy the bulk ignition issue along with other materials that will result from the existence of the former materials. Table 3.2 shows the expected peak irradiance for the gain spike and the main pulse that these materials can take without bulk melting and hence avoid bulk plasma ignition. In both of these tables, we ignore the temperature dependence of the conductivity, the specific heat, the absorption, and the density. Clearly as the temperature before the applied fluence rises there will be significant decrease in the allowed level of fluences. Tables 3.2, 3.3, and 3.4 use formulas where the initial temperature is 0°C. If the initial temperature, T_I, is high enough, this T_m

should be changed to $T_m - T_I$. For convenience, the design values for peak irradiance are also listed for these pulse elements. Only Al, Cu, Mo, and Au can satisfy the design values and hence will not cause bulk plasma breakdown.

Table 3.2. Maximum allowed incident irradiance for gain spike and for main pulse with no bulk melting and no bulk plasma ignition for a 10 μs pulse.

Material	Gain Spike I_s(MW/cm^2)	Main Pulse I_m(MW/cm^2)	Base Computation Term $\sqrt{KC_p\rho\frac{\pi}{4}}\ T_m/\alpha$ [KJ/cm$^2\sqrt{s}$]
Al	128.0	22.2	70.25
Cu	425.8	73.7	233.20
Mo	424.4	73.5	232.45
Au	232.5	40.3	127.35
Stainless Steel	18.4	3.2	10.08
Aluminum Oxide	8.5	1.5	4.65
Cu O	0.9	0.15	0.49
Graphite	6.6	1.1	3.50
Ni	7.1	1.2	3.89
Be	9.7	1.7	5.33
Peak Irradiance (design purposes)	50 MW/cm^2	10 MW/cm^2	
Time of pulse	0.3 μs	10 μs	
Fluence	15 J/cm^2	100 J/cm^2	

Table 3.3. Expected damage threshold of fluence from bulk melting for different times. Use data from Table 3.1. The equation is

$$F = \left(\frac{\pi K \rho C_p}{4}\right)^{1/2} \frac{T_m}{\alpha} \sqrt{t} \quad .$$

Copper Fluence (J/cm^2)	Gold Fluence (J/cm^2)	Time of Pulse
7.4	4.0	1.0 ns
23.3	12.7	10. ns
73.7	40.	100. ns
233	127.	1. μs
737	400.	10. μs

Table 3.4. Expected damage threshold of fluence from surface defects model for copper and gold. Use data from Table 3.1. The equation is

$$F = T_m C_p \rho d/\alpha \quad .$$

Copper Fluence (J/cm^2)	Gold Fluence (J/cm^2)	Thickness of defect, d (μm)
247.	12.4	10.0
120.	5.0	4.0
59.4	2.48	2.0
24.7	1.24	1.0
2.5	0.12	0.1

Both Al and Cu are subject to catastrophic oxidation and therefore cannot be used at the desired interface for the drone. Gold is very heavy and expensive, thus it is not an ideal material. Two possibilities appear to remain. Gold-plated copper and Mo each satisfy these bulk ignition constraints. References 7, 23, 26, 28, 29, 30, 31, 33, 34, 35, 38, 39, 41, and 42 provide evidence that the intrinsic behavior of bare copper, gold-plated copper, and Mo satisfies the implied results of Table 3.2. Therefore we conclude that these last two materials are the only candidates for consideration if we are to avoid bulk plasma ignition. By way of comparison, we show the expected damage threshold for bulk effects in Table 3.3. This is a table of bare copper and gold subjected to different lengths of pulses.

Reference 7 suggests that surface defects are the prime cause for local plasma ignition. Table 3.4 applies this model for this surface melting and shows what is the expected "smoothness" necessary for bare copper and gold to avoid local plasma ignition. Here we have assumed that any melting is the prime threshold for induced plasma ignition. To satisfy our design goals, we require that the surface remain "smooth" to at least 4 μm. This means that there can be no scratches, induced slips of crystals, or other surface defects that can show pieces of metal with thickness less than this number. The temperature dependences of the material will require the thickness of the defect to increase so the temperature rises. To attain this situation is not easy. In fact the literature suggests that these limits for smoothness are not satisfied for the 100 ns pulses of references 37, 38, and 39 for either Mo or Cu.

We eliminate Mo as an acceptable material by noting the results of references 37 and 39. In particular on page 512 of reference 39 we find that the damage threshold of gold-plated copper is near 20 J/cm^2 and that for Mo is near 7 J/cm^2. This is sufficient reason to eliminate Mo. Reference 37 suggests the polishing of Mo for a smooth enough surface is a serious problem. There is also a question about its oxide properties. There is no known data on the oxide.

Can we be sure that gold-plated copper can do the job over some useful range of the expected fluences? One expert [25] thinks that a hard enough copper that is properly polished will take the design range. He suggests that the requirement is a hardness of 40 on the (Rockwell ??) scale. Once a design is chosen, we suggest an exact written specification of the material used by AVCO be identified and compared with the conclusions we have drawn below based on the published literature and on our understanding of the issues for developing appropriate surfaces. Diamond-turned copper shows the highest threshold in references 31 and 33 for melting because it appears to be the smoothest and cleanest surface. Unfortunately, there appear to be voids in the material in both cases of the size 50 nm in diameter and 25 nm deep. Reference 31 shows that gold plating of copper which is oxygen-free-high-conductivity (OFHC) will fill these voids with gold and replace the surface with hills that have a height of 10 nm. This surface has an implied damage threshold near 48 J/cm^2. This latter fact makes it likely the plating of gold need not be too thick provided good mechanical contact is made by the plating process.

Reference 33 shows a more complex set of issues about the damage conditions on the surface of materials. They suggest that slip of the crystals in the metal shows the weakest feature of the metal and that it can be reduced somewhat by work hardening the surface (polishing) at the price that the damage threshold by melting and other features is reduced significantly.

Deciding what can be expected for our design situation is difficult since the literature is not necessarily directly comparable or exactly correct for the situations we are trying to satisfy. Before we list our suggested solutions, we list comments about various selected references to point out what they provide to help in the final decision for the appropriate fabrication of this interface:

1. Reference 3 shows that copper foil with a grating can take 4 J/cm^2 for 40 pulses in a second without plasma ignition and damage.

2. Reference 23 shows that we can expect some form of work hardening and annealing on the interface surface as it is used in the measurements. This means that the prepared surface will eventually fail to be ideal and the threshold for damage will drop.
3. Reference 23 informs us that plasma ignition is possible with a fluence as low as 0.5 J/cm^2 if there are holes in the interface plate. This implies that diagnostics using holes may not be possible for <u>any</u> practical fluences of interest. Even if the SF_6 works, there can be expected a chance for plasma ignition unless some very special surface preparation is performed on each hole.
4. Reference 7 allows the inference that it may be possible to avoid those low level plasma ignition problems by making appropriate holes with microscopic smoothness.
5. References 29 and 31 allow us to conclude that gold-plated copper has a high damage threshold--at least 20 J/cm^2.
6. References 26, 27, 30, 33, 34, 35, 38, and 39 allow us to conclude that diamond-turned surfaces have the best chance for a clean and smooth surface that will lead to a consistent damage threshold on the surface. The discussion of reference 38 suggests that high crystalline order is to be avoided on the surface. Reference 35 gives a discussion of the source of the voids in diamond-turned copper. Reference 34 contains a comment that diamond-turned surfaces degrade (oxidize) faster than polished surfaces for copper mirrors. This may be due to the turning marks on the surface.)
7. Reference 32 shows how to polish the diamond-turned mirrors. Given the conclusion about the work hardening in reference 23 and the issues raised above, this may prove to be necessary for proper preparation of the gold-plated copper.
8. References 38, 39, 41, and 42 suggest that there are difficult problems in attaining the intrinsic damage thresholds for copper and other materials.
9. To add to the problems, we include the very important fact that as the temperature goes up, the absorption of the material such as gold or copper can have a significant change in value. References 1 and 44 have curves showing such details. These results imply it is necessary to calibrate the actual interface under the nominal field conditions and make sure that the temperature of the interface does not rise too much. Stainless steel does not have as severe a problem. This issue will have to be remembered during the calibration and experimental design processes.
10. A final issue affecting construction of this interface arises from the fact that we can expect water vapor under the field conditions. References 39 and 40 suggest that this is a significant source for lowering the plasma ignition threshold and for damage to the interface because water is a strong absorber of 10.6 μm radiation. Therefore, it may be necessary for the interface material to be at an elevated temperature relative to the dew point to keep it as free as possible of water vapor. In addition, there is the possible surface contamination of the interface material by particulates in air during a flight of the drone.

In conclusion, the above issues strongly suggest that it is not possible to have a target board that will work consistently over the entire design range. It is very likely that local plasma ignition can take place when the fluence level for each pulse exceeds

20 J/cm^2. It appears possible to construct the interface so that it can take individual fluences between 10 and 20 J/cm^2 for the pulse shape under discussion and not ignite. This effort is desirable because then the SF_6 has a better chance to allow full dynamic range for the desired design conditions of 120 J/cm^2.

3.3 Possible Solutions to this Stage

3.3.1 Accept the ignition of plasma

Given the collection of problems in development of the interface material for the target board, perhaps the best solution is to accept the plasma. In this case we can use various interface materials, including either polished or roughened Al, stainless steel, and Mo. Here we accept the range where no plasma is ignited and then consider different analyses for those conditions when the plasma is ignited. The molybdenum becomes a very attractive candidate for use because it has a very high threshold for bulk damage. Because Mo is very hard, the threshold for the plasma ignition can be expected to hold consistently over the entire sequence of the repeated pulses. Reference 6 suggests this is not true for Al. This could be an important issue in the measurements performed at the field site. The disadvantage has already been mentioned, namely the desired beam profile measurement becomes impossible when the plasma is ignited.

3.3.2 Use a gold-plated Cu plate with holes to sample beam

Here we accept the plasma ignition and just measure the beam accepted by the holes of 1 cm diameter during the initial period before the plasma blocks each hole. Here we must assume that the pulse shape is known and that these truncated measurements of fluence or of the irradiance at some time like 1 μs after the start of the pulse can be useful measurements. This approach may prove necessary if the shield of SF_6 in front of the target board fails and if it is desirable to measure beam profile under the plasma ignition conditions. The prime disadvantage is that it may imply very fast electronics and complex analysis.

In this case wedges of NaCl could now be used after the interface plate to get various beams of 1 cm diameter some of which could go directly to thin film detectors and/or to calorimeters without damaging them [49]. It would be necessary to develop the means to confirm the ignition of the plasma at each hole so that the measured irradiance or fluence could be appropriately corrected. Change in pulse shape due to cutoff would be one way to confirm plasma ignition.

It is also possible to use a set of specially polished and tested gold-plated thin (1 mm) disks of copper as the absorbing material with SF_6 to keep down the chance for plasma ignition. In this case the environment can be kept clean and conditions will not be as harsh and unpredictable as will be the conditions on the outside of the drone. Of course, the plasma could produce some form of contamination if there is insufficient over-pressure to be sure the vapor and other products are kept out of the drone's interior.

Also, a set of calorimeters with SF_6 and acoustic transducers could be used if the holes are present and a means is available for plasma detection.

3.3.3 Ablation of material as a measurement tool

Here we accept that a material such as graphite or plexiglass can be used as an ablator on a pulse by pulse basis. The advantages are that the plasma is now accepted as part of the transfer process and would be calibrated into the ablation rate. To reduce the level of convolution between the sampled elements of the beam profile, the ablated material would be a bunch of rods sticking out of the side of the gold-coated copper interface. The sides of the rods would be plated with a thin coat of copper so that the rods are not damaged and so that the chance of plasma ignition is minimized between rods. The ablation would take place on the tip of the rod. If the length of the rod could be measured on a pulse by pulse basis, this technique may be a viable measurement process. (We have done some preliminary designs for such a system and will discuss them if this technique proves necessary.) The prime disadvantage of this technique is that an extensive calibration process would be necessary because there is no data that could be used with confidence to infer what will happen during the ablation process over the desired range of fluences. Again, the uncertainty of plasma ignition affects the expected accuracy of these measurements. (R. Conrad has designed and pantented an instrument that uses the fact that ablation of plastic causes visible light emission. This light is proportional to the ablation rate.)

3.3.4 A thin sheet of gold-plated copper that is super-polished

Here we try very hard to get the minimum chance of plasma ignition. We hope that the effects of the environment on the target board are small enough so the board can be used enough times to make it cost effective and that if scratches develop, they can be removed by re-polishing and possibly replating the board or even re-turning if it is a diamond-turned plate. The advantage of this approach is that we will extend the range for beam profile measurements into fluences where plasma ignition usually obscures the results. This means the measurements will be of the best quality. The disadvantage of this approach is the need to do research and development to learn how to extend the range. We are not certain that there can be developed a thin sheet of such material with the necessary hardness and stability to avoid all the problems caused by the laser pulses and the environment [45, 46]. Again, calibration of the resulting material becomes necessary. The size of the material approaches the size of large mirrors. This implies significant costs to get the desired conditions.

3.3.5 A gold-plated copper sheet that is super-polished once

Here we get the best material we can have today, namely rolled copper of OFHC quality with the hardness implied by reference 25. We make sure that there are no voids in the material. We make sure that the level of crystalline order is a minimum for both the copper and the gold. Next, we polish the material to the best possible level without regard to surface figure. We eliminate only the surface scratches. We recrystallize to a depth of 100 μm by flash heating with a laser and repolish as necessary [46]. We make very sure that the surface is very clean before the gold coat is put on. We use a moderate electric current

in the plating process to make a thick and uncloudy coating of gold [45]. The coating would be near 4 μm thick. This surface could be polished by the techniques suggested in reference 32 so that we have a clean and polished surface with minimum scratches. We would use a quantitative scan of the scatter to infer the status of this plate after each use of the drone. We watch carefully for effects defined by references 47 and 48 to see if the surface changes significantly with time.

We will only apply fluences less than the tested damage level to this plate, accepting the test damage level as our restriction on this interface. If the plate can be made so that it can take the entire design range of fluences and if the surface can be protected by the cover on that drone so that no scratches or surface contamination can take place during a run and that which develops can be removed by the cleaning process of reference 32, then we have a good solution to this stage. If any of these conditions fail to apply, then the applied fluence range will be reduced to allow the plate to survive and to minimize the replacement cost of this apparatus.

3.4 Suggested Solution

As you can see from the discussions in this section, the issues for developing the appropriate interface to sample the laser pulses are extremely complex and at this time subject to many unknown conditions. There are too many uncontrolled elements at this time in mirror damage studies to easily apply the results to repeated laser pulse processes. Therefore, our suggestions here are guesses using our understanding of the state of the art. We have tried to use the best available information that appears consistent. This section has indicated all known issues and has proposed what should be done in 3.3.4 and 3.3.5. To sort out the optimum choice for dealing with the copper or any other metal would require research and development. Given these qualms, we now present our best guess.

Use the sheet of gold-plated copper (OFHC) with the necessary work hardening and recrystallization so that the surface of the copper is stable to repeated laser pulses. It is very necessary to avoid the creation of defects on this surface which have thickness less than 4 μm. By avoiding the voids, by making sure the grains are very small to avoid the slip effects [47, 48], by recrystallization with a pulsed laser and by polishing as necessary so the surface is stable to the laser pulses and retains the required "smoothness," the plate can be now used as a target board. Once this is done, then a layer of gold can be electroplated on the copper to a depth of at least 4 μm to protect the copper surface from oxidation and to permit a proper polishing of the gold. This surface may also have to be recrystallized and polished to finally stabilize it to the laser pulses and to the "smoothness" conditions. Once this plate has been constructed, then we believe it will be a stable absorber of the laser radiation and hence can be calibrated to permit accurate beam-profile measurements. We also believe that the damage threshold will easily exceed the 20 J/cm^2 and probably will reach the values implied by reference 31, which is about 50 J/cm^2. If our understanding of the plasma breakdown process is complete, we can expect to have an interface that can take the 120 J/cm^2 design limit as long as the total temperature rise of the

substrate* is less than 300°C and we can get rid of the metal flakes with less than 4 μm thickness.

In any case, our suggested solution is to build one such plate and accept the damage threshold as the design limit for measurements. We then use SF_6 as the means to extend the fluence levels beyond the measured damage threshold.

Finally, we suggest that this plate must always be maintained above the dew point or in a water-free environment and that this plate be mounted to accept the expansion from heating without any strain. A change of 400°C from 0°C implies a 0.66 percent change in length of copper. This is almost 2 mm along the 30 cm length.

3.5 References

[1] A. K. Ghosh, Review on High-Power-Laser Damage to Material II, page 279, RCA Review, Vol. 35, (1974).

[2] See reference 1 of section 2.

[3] See reference 2 of section 2.

[4] See reference 3 of section 2.

[5] See reference 4 of section 2.

[6] S. Marcus, J. E. Lowder, and D. L. Mooney, Large-Spot Thermal Coupling of CO_2 Laser Radiation of Metallic Surfaces, page 2966, Journal of Applied Physics, vol. 49, No. 7, (1976).

[7] C. T. Walters, R. H. Barnes, R. E. Beverly, An investigation of Mechanisms of Initiation of Laser-Supported-Absorption Waves, AD-A024496 (1975 Sept.).

[8] D. A. Reilly, P. S. Rostler, Pre-breakdown Laser Target Vaporization of Enhanced Thermal Coupling, AD-A009297.

[9] C. T. Walters, An Investigation of Mechanizms of Initiation of Laser-Supported-Absorption Waves, (1975 Jan.) AD-A024550.

[10] A. N. Pirri, R. C. Root, P. K. S. Wu, Analytical Laser Material Interactions Investigations, Volume 1-Theory, AD-B023053L.

[11] Private communications with C. T. Walters (Battelle) and with R. G. Root (Physical Sciences, Inc.).

[12] P. J. Klass, Pulsed Laser Eyed for Extended Range, page 56, Aviation Week and Space Technology (August 28, 1978).

[13] A. N. Pirri, R. G. Root, and P. K. S. Wu, Plasma Energy Transfer to Metal Surfaces Irradiated by Pulsed Laser, page 1296, AIAA Journal, vol. 16, No. 12, (1978).

[14] C. T. Walters, R. E. Beverly, III, and T. J. Negrelli, Exploratory Development of Laser-Hardened Materials and Measurement of Laser Beam Parameters and Material Response to High-Power Laser Radiation, vol. I, (Dec. 1975) AD-A026831).

[15] Same title as reference 14 except it is volume II, AD-A026915.

[16] J. F. Ready, Investigation of Material Damage, (1977) AD-A043437.

---

* We have been informed that copper can have significant vapor pressure in a high vacuum system when the temperature of the material gets as high as 400°C. If the suggested cycling in section 10 from 100°C to 400°C show no reduction in damage threshold, then this issue is insignificant. It is possible gold will diffuse into the copper.

[17] J. F. Ready, Investigation of Material Damage: Pressure Pulses Produced by Carbon Dioxide Laser Radiation, (1976) AD-A023047.

[18] T. J. Magee, J. Peng, R. A. Armistead, Laser Damage Phenomena in Materials, (1976) AD-A037163.

[19] S. S. Cunningham, W. T. Lauglin, The Surface Absorption of Unpainted Alloys at 10.6 μm, (1974) AD-776763.

[20] J. L. Smith, Target Damage Studies with a Pulsed CO_2 TEA Laser Facility, (1974), AD-A008313.

[21] S. Marcus, J. E. Lowder, S. K. Manlief, Laser Heating of Metallic Surfaces, (1974), AD-A028580.

[22] L. A. Young, J. A. Woodroffe, E. R. Bressell, Laser Effects Assessment Program, (1978), AD-B026974L.

[23] I. P. Shkarofsky, Review on Industrial Application of High-Power Laser Beam III, page 336, RCA Review, Vol. 36, (1975). See page 365 for discussion of annealing effects and for shocking the material with a laser.

[24] Private communication with J. A. Woodruffe (AVCO).

[25] Private communication with George Theophenis (AVCO).

[26] D. L. Decker, M. J. Soileau, J. O. Porteus, and J. M. Bennett, Surface, Optical, and Laser Damage Characteristics of Diamond-Turned Mirrors, page 153, Laser Induced Damage; 1976, NBS Special Publication 462.

[27] J. O. Porteus, M. J. Soileau, and C. W. Fountain, Character of Pulsed Laser Damage to Al to 10.6 μm Infrared from Single-Crystal Targets in Vacuum, page 165, same publication as reference 26.

[28] J. Hayden and I. Liberman, Measurement at 10.6 μm of Damage Threshold in Germanium, Copper, Sodium Chloride, and other optical materials at levels up to 10^{10} W/cm^2, page 173, same publication as reference 26.

[29] R. Gibbs and R. M. Wood, Laser-Induced Damage of Mirror and Window Material at 10.6 μm, page 181, same publication as reference 26.

[30] F. Haessner, W. Seitz, Laser-Induced Dislocation Structures in Copper Single Crystals, page 16, Journal of Material Science, vol. 6 (1971).

[31] S. Sharma, R. M. Wood, and R. C. C. Ward, Measurement of Mirror and Window Characteristics for Use with 10.6 μm Lasers, page 183, Laser Induced Damage in Optical Materials; 1977, NBS Special Publication 509.

[32] R. W. Parks, R. E. Sumner, and R. E. Strittmatter, Polishing Single Point Diamond Turned Mirrors, page 196, same publication as reference 31.

[33] J. O. Porteous, C. W. Fountain, J. L. Jernigan, W. N. Faith, and H. E. Bennet, Pulsed-Laser Stress Phenomena on Highly Reflecting Metal and Allow Surfaces, page 204, same publication as reference 31.

[34] D. L. Decker and D. J. Grandjean, Physical and Optical Properties of Surfaces Generated by Diamond-Turning on an Advanced Machine, page 122, Laser Induced Damage in Optical Materials: 1978, NBS Special Publication 541. See comment on page 125 relative to the micro-cracks and voids. Also see reference 35.

[35] D. L. Decker, J. M. Bennett, M. J. Soileau, J. O. Porteus, and H. E. Bennett, Surface and Optical Studies of Diamond Turned and Other Metal Mirrors, page 160, Optical Engineering, vol. 17, No. 2, (1978).

[36] J. B. Arnold, T. O. Morris, R. E. Sladly, and P. J. Steger, Machinability Studies of Infrared Window Materials and Metals, page 324, Optical Engineering, vol. 16, (1977).

[37] S. M. Wong, G. Krass, and J. M. Bennett, Optical and Metallurgical Characterization of Molybdenum Laser Mirrors, page 132, same publication as reference 34.

[38] J. O. Porteus, D. L. Decker, J. L. Jernigan, and W. N. Faith, Evaluation of Metal Mirrors for High Power Application by Multi-Threshold Damage Analysis, page 84, IEEE Journal of Quantum Electronics, vol. 13, No. 9, (1977).

[39] J. O. Porteus, J. L. Jernigan, and W. N. Faith, Multithreshold Measurement and Analysis of Pulsed Laser Damage on Optical Surfaces, page 507, same publication as reference 31.

[40] V. I. Kovalev, F. S. Faizullov, Investigation of Surface Breakdown Mechanism in IR-Optical Material, page 318, same publication as reference 34.

[41] G. T. Johnson, S. H. Mersch, Large-Spot Pulsed Damage Tests of Mirrors, UDRI-A-141 (1979).

[42] G. T. Johnson, R. A. House, D. L. Mullen, SRAT Single-Pulse Mirror Damage Tests, UDRI-A-137 (1978).

[43] JANAF RP VEH Meeting in June 22, 1979.

[44] K. Ujihara, Reflectivity of Metals at High Temperatures, page 376, J. Applied Physics, vol. 34, No. 5, (1972).

[45] To satisfy MIL-G-45204B, Amendment 2, Type IID, we should use a plating compound of gold with 1 percent cobalt. This is the hardest plated gold. The question here is: Can this mixture have an adequate damage threshold compared to the pure gold? A test will have to be made.

[46] Private communication with David Read (NBS). He suggests that the copper will have to be subjected to a recrystalization stage for a time period equal to ten times that period the pulses are to be applied. This implies a 100 μm depth in copper for 100 μs pulses. The gold plate will behave as a thin film on the copper, therefore, the gold's crystalline structure is primarily determined by the behavior of the copper surface and not by the character of the gold.

[47] B. A. Rogers, The Nature of Metals. See page 70 for structure of copper ingot, page 169 for fiber structure of cold rolling by 97 percent reduction, page 171 for discussion of recrystallization effects. Note the room temperature processes on recrystallization of rolled copper. This book is published by The American Society for Metals, Iowa State College Press, Ames, Iowa, in 1957.

[48] R. C. Fullerton-Batten, A. Baymor, and W. O. Fauson, Using Beryllium Instead, Part I in Optical Spectra, July 1979, page 49; Part II in Optical Spectra, August 1979, page 50. They discuss the construction of dimensionally stable mirrors. This point may relate to this problem of prompt plasma ignition.

[49] See reference 26 of section 2.

4. Dealing with the Absorbed Heat to Get Beam Profile Measurements

This section is organized differently from the previous two. Here we deal with a series of technical decisions on the structure of the target board, on the number of allowed pulses in a given measurement sequence, and on the spatial sampling structure of the heat distribution at the back surface of the target board. Because these decisions are somewhat arbitrary, yet are unique in the sense that some decision has to be made before the rest of the equipment can be built, we develop the specifics here and just give a reason why the values for design were taken rather than attempt to show many possible solutions.

4.1 Purpose of this Stage

Here we select the necessary thickness of the target board, the allowed number of laser pulses during a measurement sequence, the preparation of the back surface of the target board for optimum thermal emission, the spatial sampling for the detectors, the temporal sampling of each heat pulse, and finally the details of the calorimeter disks cut into the back of the interface plate. This discussion shows what are the issues in design by generating a specific example.. If it proves necessary to change some of the constraints suggested, then some of the elements of this board will also change.

4.2 Selecting the Necessary Thickness of the Copper Plate

Table 4.1 shows the temperature rise per pulse in the copper plate neglecting any transverse heat flow, assuming that the gold on the front of the target board has an average absorption of 0.03 for the entire potential temperature change of 300°C (as already discussed in section 3) and using the maximum and minimum design fluences as a function of different thicknesses of the target board. We see that the dynamic range of the temperature changes per pulse can be from 20 m°K to 10°K. If we assume that a practical sampling rate for temperature measurement will be about every millisecond (see the timing issues in the electronic section), then it is desirable to choose the thickness of the plate to be thin

Table 4.1. Selecting Thickness of Copper Plate Using Formulae $\Delta T = \alpha F/(C_p \rho d)$, and $\tau = C_p \rho d^2/(\pi^2 K)$.

ΔT (K)	Thickness d(mm)	Applied Fluence $F(J/cm^2)$	Fundamental Time Constant τ(ms)
10.5	1	120	0.89
0.087	1	1	0.89
5.2	2	120	3.58
0.044	2	1	3.58
3.5	3	120	8.05
0.029	3	1	8.05
2.6	4	120	14.31
0.022	4	1	14.31

enough so that the second time constant (this is 1/4 the fundamental time constant) will be no larger than 1 ms. This implies that the plate thickness where temperature measurements are made should be no thicker than 2 mm. In this way we will have single exponential time behavior. In those areas where the temperature is not being measured, the thickness should be large enough to support as many pulses as necessary under the worst conditions while minimizing the warping process. Further, the plate should be flexible for bolting down to the drone and getting a reasonable curvature for defocusing the laser beam. For a plate of 23 cm by 33 cm, 3 or 4 mm is about as thick as needed for heat loading and still have adequate flexibility for bending. We presume in this discussion that the thickness will be 3 mm. This is about 1/8 inch which should be a commercially available thickness from cold rolling of sheet copper.

We set the active dimensions of the plate to be 20 cm by 30 cm as it can fit on the drone's front payload section which has dimensions 23 cm by 60 cm.

4.3 The Allowed Number of Laser Pulses for a Run

Table 4.2 shows what is the allowed number of pulses under two extreme limits assuming that the design fluence level has been deposited on the interface. If there is no beam jitter, the number of pulses that are allowed would be 57 for the area where temperature measurement are to be made and would be 85 in remaining areas of the copper plate. The radial-heat conduction will allow some adjustment of this pulse number. For large spot-diameter-laser pulses, this adjustment can be expected to be of no consequence, therefore, a design limit for a run would be no more than 57 pulses at the 120 J/cm^2 fluence level if there is no beam jitter. To the extent the beam jitter implies the overlap between laser pulses is less than 20 percent or so, then the statistics model can be applied. In this case, the limit on the number of pulses is greater than 1600.

Table 4.2. Allowed number of pulses for maximum fluence using (1) no statistics and (2) gaussian statistics for each thickness.

Number of Pulses Without Statistics $N_m = 300K/\Delta T$	Number of Pulses With Statistics $N_g = N_m^2/2$	Plate Thickness (mm)
28	392	1
57	> 1600	2
85	> 3600	3
115	> 6600	4

4.4 Preparation of the Back Surface for Optimum Thermal Emission

Those areas, where the temperature is to be measured by a detector that is not in contact with the plate, should have as high an emissivity as possible. To get the high emissivity, either a black paint, gold black (best), or emulsified carbon will do the job. We must keep in mind that this layer will reduce the actual temperature radiating to the detector, therefore, this layer should be very thin.

Those areas, where no temperature measurements are to be made, should have minimum emissivity so that the electronics inside the drone do not get unnecessarily heated. This can be done by using a shield between the interface plate and the electronics. In this case, the shield would have holes to allow the detectors to see the appropriate areas.

4.5 The Spatial Sampling for the Detectors

Selecting the proper spatial sampling procedure on the back of the plate is difficult. If scanning type techniques can be applied, then the limiting criteria for sampling density is the scan rate of the technique. Most commercial scanning techniques have a scanning rate around 1/60 second or slower for each frame. This is too slow if we are to examine details of a heat pulse at the expected millisecond rate. A second disadvantage of the scanning technique is the skew in time of the beam profile induced by the scanning process. If the sample and hold technique works properly within the vidicon then this may be minimized. Further issues about the scanning system will be discussed in the detector part of this report. Here we presume that scanning will not be used because the dynamic range of temperatures is too much for such devices (20 m°K is not seen by these devices), the skew is not desired, the optics for fitting the image of the back of the plate takes up too much of the drone's interior, and there is needed a development of an appropriate array of pyroelectric detectors in the vidicon for efficient use of the TV scan technique at higher scan speeds.

Given the above discussion, we now assume that the technique for sampling the back of the plate will be an array of detectors. Commercial detectors have cans which will allow a density of about one every centimeter. This would imply for a 20 cm by 30 cm active area, about 600 detectors. This is a very large number of electronic channels and therefore is expensive. We need to identify how few detectors we can use and yet get sufficient accuracy for our beam profile measurements.

We now list the issues that can set the number of such detectors.

1. The expected deconvolution effects due to plasma ignition will have dimensions around 3 cm radius. The velocity of sound is near 3×10^5 cm/s.
2. The heating of the SF_6 can imply deconvolution effects around one centimeter radius. The velocity of sound may reach 10^5 cm/s.
3. The details of interest about the beam profile are primarily an average and variance of the beam parameters within a run or between runs and not of the actual details in a single pulse. Thus we need only as much detail as is necessary to get convergence in estimating the averages.

4. Choosing a mathematical model that can represent the shape of the fluence distribution will affect the apparent accuracy for the beam parameters. There are three practical models. One model assumes a simple linear interpolation between the measured data and assumes that there is no error in the individual measurements. The error estimates are determined by using comparisons between different pulses within and between runs. A second model assumes that there is smoothness in the fluence distribution because it is at the far field of the optics. In this case we use cubic spline techniques to fit the measured data. (See section 8 on modeling.) Again the errors are presumed to be estimated comparing the results between pulses. A third model assumes that the shape of the fluence is approximately described by sinc functions for each of two transverse dimensions. Thus we have

$$F(x,y) = F_0[\text{sinc}[a(x-x_0)]\text{sinc}[b(y-y_0)]]^2$$

as the fluence shape. The x and y are referenced relative to the center (x_0,y_0) of each pulse and the a and b are adjusted to get an estimate of the spot size of the fluence distribution. The F_0 is adjusted to the energy in the pulse. (Skew in the fluence distribution is ignored here.)

5. The choice of measurement technique should be insensitive to the models because the measurement situation will not necessarily be as expected once the actual laser system is operational. Therefore the key issue for selection of the number of detectors is to choose enough for data details and to expect the computer with appropriately modified software to use models such as the ones indicated in (4). No preprocessing of data is proposed within the drone because we need complex computer algorithms.

Given the above issues, we set the number of detectors to be as large as the budget will allow and to decide somewhat arbitrarily that this number should be at least a ten by ten array or one every 3 cm in the horizontal direction (x coordinate) and one every 2 cm in the vertical direction (y coordinate). This level of sampling would imply a worst case determination of the center of the peak fluence to an accuracy of ±1 and ±1.5 cm respectively. The position of the centroid of the fluence will be at least this same accuracy or better. The actual accuracy estimates for both positions depend on the model used.

4.6 Temporal Sampling of each Heat Pulse

The sampling rate for the time dependent details of a detector is determined by the time constants of the analog electronics, the detector, the interface plate, and the digital electronics. We have already set the key time constants of a heat pulse to be in the 1 to 10 ms range, therefore, it is reasonable to set the time scale of all electronics to be at the 1 μs to 1.0 ms level. There is not much point to making them have speeds significantly faster than the details of the heat pulse. Because we want to allow a high rep rate for the laser pulses, so the design will work as the laser system changes, we choose a millisecond for data sampling with the provision that some millisecond periods of sampling will have no actual data storage. In this way we can conserve the data memory, simplify the

structure of the electronics and have maximum flexibility in the sampling of each heat pulse. For example:

1. One strategy would be to start the process with a measurement of the heat pulse as seen by a detector at the time (within 20 μs) of the incident laser pulse. Wait for 3 or 4 ms to allow the high order exponential features of the heat pulse to decay and then measure at the next 3 or 4 ms intervals.
2. A second strategy would be to use the earlier 3 or 4 ms and therefore measure the signal around the peak of the signal.

4.7 The Calorimeter Disks Cut into the Interface Plate

Here we discuss the issues for construction of the disks into the back of the interface plate. There are two competing issues:

1. By just accepting a flat plate of 2 mm thickness everywhere, the cost of construction will be a minimum. This configuration is easier to use since there is no unique location for the selected heat pulse structure. Unfortunately, the polishing and surface preparation on the front surface of the plate may require a thicker plate than the 2 mm. It may have to be 3 or 4 mm thick. In this case, it becomes very desirable to have the calorimeter disks cut into the plate.
2. In the calibration process, there is advantage to knowing the expected temporal shape of the heat pulse from first principles. By cutting rings into the back of the interface plate to create discrete heat modes, we get single-exponential temporal behavior in our pulse shape provided the electronics do not significantly distort the measured values. This known mode behavior can be used in computer program to estimate errors in measurement of a given heat pulse. For example, the change in the computed time constant of the exponential could provide a consistency check of the absolute temperature in the individual disk.

   Figure 4.1 shows how the disk cut could be made so that the single pulse heating will not damage the plate at the cut and so we can get a signal with the exponential time dependence. Table 4.3 shows that a radius of 2 or 3 mm gives a time constant in the tens of milliseconds range. This size of disk is consistent with an interval between pulses near 10 ms. For rep rates near 10 per second, we could use 5 mm radius disks.

For a first design effort we suggest that two rolled commercial grade plates of copper be obtained. One plate would be about 1.5 mm (1/16") thick with no disk cuts and the second plate would be about 3 mm (1/8") thick with disk cuts as suggested in figure 4.1. Each plate would then be subjected to multiple polishing and recrystallization cycles to see how well the front surface can be stabilized. In addition, these plates will have to be bent slightly to simulate the resulting strains. In order to minimize costs, neither plate will not be gold plated until it is clear by these tests* which plate will show no local plasma

* Note that oxidization must be avoided by keeping the plates in an oxygen-free environment.

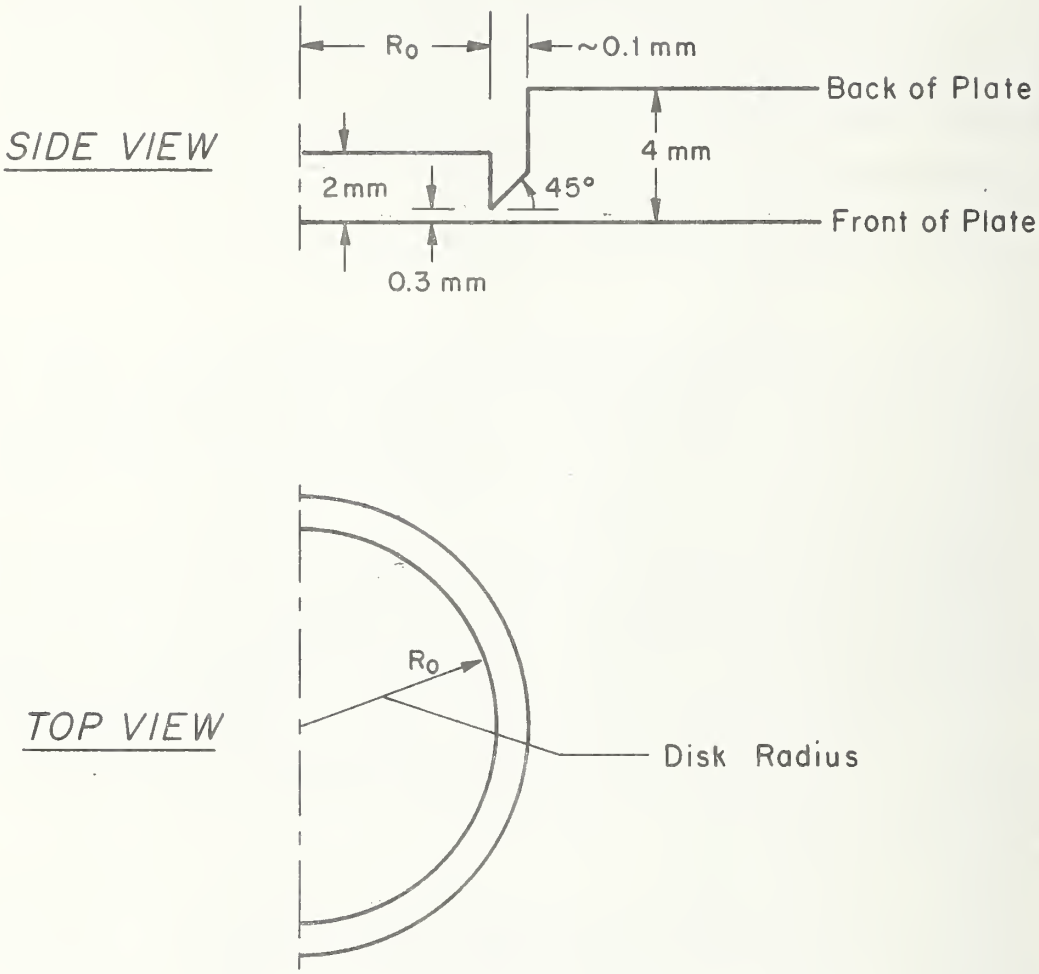

Figure 4.1 The cross section of the disk cut into the target board.

Table 4.3. Radius of copper disk versus time constant for lowest order radial mode. $\tau = c_p \rho R_o^2/(\xi^2 K)$. Here $\xi = 2.4$ is the first zero of Bessel function J_o.

Disk Radius R_o(mm)	Fundamental Time Constant τ (ms)
1	1.53
2	6.13
3	13.8
4	24.5
5	38.3

ignition at the required design level. To decide how large these test plates should be, we will depend on the advice of the persons who do the polishing. Our suggestion is that these plates should be at least 8 cm by 12 cm so the issues of large area polishing can be tested, and so we can confirm if the copper (OFHC) can be obtained that is homogeneous over this area in crystalline structure, in the absence of voids, etc.

5. Detector System

5.1 Purpose

This system is to read the temperature profile of the back side of the target board.

5.2 Problem

The system is to read the temperatures of the backside of a plate 20 cm x 30 cm. The resolution will be such as to divide the area into 100 pixels. The range of temperatures of the plate will be from 100°C to 400°C. The individual pulses to be read will cause temperature rises from 0.04°C to 5°C determined from the incident energies and an assumed target board thickness of 2 mm. All 100 elements are to be read at rates up to 1000 per second.

5.3 Solutions

There are two approaches to reading the temperature profile of the backside of the target board. Individual thermal sensors in intimate contact with the surface could be used, or the temperature can be sensed from power emitted to detectors separated from the surface. The first approach avoids signal losses due to projection optics and avoids the complications of the temperature to the fourth power nonlinearity of thermally emitted

power. The second approach avoids difficulties, that may occur in changing target boards, due to inconsistent thermal contacts with the sensors.

Considering the intimate contact sensors, many devices are commercially available. There are number of thermocouples that cover the 100°C to 400°C range. However, an absolute calibration to 0.004°C (10% of 0.04°C) is very unlikely. Commercially available thermistors give much greater voltages at levels of impedances more compatible with inexpensive amplifiers. The contacting thermistors may also avoid the reference junction requirements of the thermocouplers; however, both systems will require considerations to avoid thermally caused drifts in the electronics. The range of readily available thermistors may be limited to temperatures far below 400°C. With either thermocouples or thermistors it must be demonstrated that a design including the amplifying electronics could be created that would have the bandwidth, temperature ranges, and resolutions required. To avoid having the expense of another sensor array for each target board, it would be preferable to be able to remove and attach this array to many boards.

For the radiation detection sensors we can go into more detail [1].

There are a number of ways to read the radiation patterns: (1) a single detector using optics and mirrors to scan over the two dimensions of the target, (2) a linear array that is electronically multiplexed for one axis scan and a moving mirror for the second axis scan, (3) an infrared vidicon camera with two dimensional electron beam scanning, (4) an array of individual detectors, one for each pixel, that electronically is multiplexed for the readings of each detector. There are commercially available systems using each approach. However, we know of no infrared system that is designed to read 1000 images a second. In addition, the best systems, operating at relatively low frame rates, claim temperature resolution of 0.1°C. In the case of interest, it is desirable to read an increment of 0.04°C with some precision. Since we have not found the data for a commercial system that will satisfy the conditions of the posed problem, we will attempt to determine if such a system is feasible.

The conditions of the problem must be converted into parameters typically used in evaluating infrared detectors.

Since the radiated power is a nonlinear function of the temperature, i.e., increases with the fourth power of the absolute temperature, we need to know both the changes in emitted power and the absolute temperature of the target.

First, we express the temperature changes as emitted power per unit area. From a 100°C target temperature and a 0.04°C rise, assuming an emissivity of one, we calculate an increase in power of 4.7×10^{-5} W/cm^2. At the other extreme of 400°C and a 5°C rise per pulse we have an increase in thermal emission of 0.035 W/cm^2. This gives a range of 745:1 for the increments in temperature to be measured. For a 10 percent measurement at the lower end we will need a total dynamic range of about 7,450:1 for the increments in power. If the full range of 100°C to 400°C is divided into 0.004°C increments (0.04°C to 10% accuracy), there are 75,000 temperature intervals. Taking into account the fact that the emitted power goes as the fourth power of the temperature, and assuming a linear electronic system, dividing the whole power range by the smallest increment in power gives us approximately another

factor of 10, making a total of 750,000 intervals. It is unlikely that there exists a single linear detector-electronics system that would cover this full range without changing some components within the range. The preceding points may lead us to a compromise for the final practical system.

Now consider a single detector, mirror scanning system. If 1000 readings per second of 100 elements are to be taken the single detector must give readings at a rate of 10^5 per second. Assuming a 10-90 percent response time of 10^{-5} seconds, to allow each reading to come within about 10 percent of its true value, the system will need a bandwidth of at least 3.5×10^4 Hz. At the low power increments where 4.7×10^{-5} W/cm^2 is emitted, a 10 percent measurement will require a signal to noise of about one at a level of 4.7×10^{-6} W/cm^2. If fast f/1 optics is used, allowing for some reflection losses, the power density at the detector may be reduced by a factor of 20 to a level of 2.4×10^{-7} W/cm^2. Now the power collected by the detector will be proportional to its area, but there will be limitations on the detector size dictated by the limits in size of the optics, the costs, and the device physics. Letting A be the detector area in cm^2, for the above bandwidth, the noise equivalent power (NEP) of the detector will have to be lower than $1.3 \times 10^{-9} \times A$ W Hz$^{-1/2}$. This implies a detectivity, D*, greater than $7.8 \times 10^8 \times A^{-1/2}$ cm Hz$^{1/2}$ W$^{1/2}$. For a practical 1 mm^2 area detector this gives a D* greater than 7.8×10^9 cm Hz$^{1/2}$ W^{-1}. An ideal, background limited detector for 300°K will have a D* of 2×10^{10} cm Hz$^{1/2}$ W^{-1}. Practical devices will have lower D*'s. In fact, it is very unlikely that there exists a room temperature broadband thermal detector that has a D* above 10^9 cm Hz$^{1/2}$ W^{-1} for modulation frequencies of 100 Hz. For a system to operate with a bandwidth of over 10^4 Hz there is no room temperature detector that will have the required D*. If we accept cryogenic cooling of a semiconductor detector, it is possible to obtain detectors that, when viewing a 300°K background, will exhibit D*'s of a few times 10^9. (Published data for D* is usually given for specific wavelengths or 500°K sources and one must estimate the D* for looking at a 100°C source.) From the above considerations the single detector mirror scanning system to read the changes in temperature is marginally possible if cryogenically-cooled detectors are acceptable.

In addition to the noise equivalent power considerations, for the above single detector system to work we have to create a mirror scanning system that will generate 1000 frames per second. This may be a formidable task not only because we have to synchronize on the laser pulses because of the speeds of moving parts that would be required, but also because of the space limitations in the drone for the instrumentation. In addition, there will probably be other reflection losses and sources of noise generated by the scanning system. Unless we compromise on the temperature ranges to be measured, it is unlikely that this approach using a single detector will work.

The second approach using a 10 element linear array for one axis and a mirror for the other axis could gain us a factor of 3 for the required NEP because we could get by with 10 times less bandwidth. However, we still have most of the problems stated above.

The vidicon approach, in principle, appears ideal because the scanning mechanism is simple, very high scan rates are possible and synchronization is easy. One also gains in

that each pixel of the image can accumulate incident energy for a large fraction of the frame interval. This contrasts with the single detector approach where the energy for each pixel would be collected for 1/100 of the frame interval. However, there are other factors that limit the minimum resolvable temperature and spatial resolution stated. Pyroelectric vidicons have achieved 0.1°C minimum resolvable temperatures at low frame rates, but we need a 0.004°C minimum resolvable temperature at a high frame rate. There are other factors such as susceptibility to electromagnetic interference (EMI) and acoustic noise for which we do not have sufficient data for any evaluation.

We will now look at the fourth approach, a two-dimensional array of individual detectors. With this system each pixel can achieve the noise equivalent temperature, or noise equivalent power, of an individual detector. The period to collect energy should be at least as good as the ideal vidicon. Although the multiplexing readout electronics is more complicated than that for the vidicon, it is reasonably straightforward. Sychronization should be easy. It just has to be shown that one can measure the temperature profile with sufficient accuracy.

For this approach we will take readings at an interval of 10^{-3} seconds. This implies a required bandwidth of about 350 Hz. Following the same arguments given for the single detector mirror scanning system our NEP or D* requirements are relaxed by a factor of 10. Continuing to assume f/1 optics, this leads us to require an NEP/A ratio less than 1.3×10^{-8} W cm^{-2} $Hz^{-1/2}$ or D* $A^{1/2}$ product greater than 7.8×10^{7} cm^{2} $Hz^{1/2}$ W^{-1}. For a 1 mm^{2} detector this implies a D* greater than 7.8×10^{8} cm $Hz^{1/2}$ W^{-1}. At these levels cryogenically-cooled detectors clearly have sufficiently low noise equivalent powers. We would prefer to use an ambient temperature detector. A "space qualified, independently verified" room temperature pyroelectric that is of sufficient size and operates at 350 Hz has been reported [2] with a $D^*A^{1/2}$ of approximately 9×10^{7}. This $D^*A^{1/2}$ would still be a marginally acceptable value.

We can possibly gain over a factor of ten in signal by modifying the collecting optics and increasing the detector areas. Instead of the f/1 optics we may use a simple, proximity coupling of the radiation from the target board to the detector. We can also add reflective surfaces, as part of the radiation shielding mentioned earlier, to couple more radiation onto the detector. The maximum possible radiation density at the detector would be equal to the power density emitted from the target board. This "optics" is possible with the 100 element array where the detectors are spaced such that they are spread out to cover the same area as the target board. The detector area can also be increased. If technically possible without reducing the D*, 2×3 cm^{2} detectors could be used to collect the maximum possible signal. At best we would gain a factor of 20 from the optics and 24 from the increased area to reduce the D* requirement to 1.6×10^{6} cm $Hz^{1/2}$ W^{-1}. This lower D* value opens up a number of possible detectors [3].

Now that it appears that we are approaching possible solutions to the low-level measurements we will consider other factors for some specific detectors.

We can estimate an NEP/A ratio for fast bolometers. What is actually needed is an NEP/A for the complete dc to 350 Hz system including detector and amplifying electronics.

The NEP/A ratio must be less than 4.7×10^{-6} W cm^{-2}. Normalizing to a one Hz bandwidth the NEP/A ratio must be less than 2.5×10^{-7} W cm^{-2} $Hz^{-1/2}$. Nanosecond response time bolometers have been made with an NEP/A of 10^{-5} W cm^{-2} $Hz^{-1/2}$ [4]. The speed of these devices was very good but the NEP/A was too high. Taking optimum inferences from reported data [2], thermistors with time constants of 1.9 milliseconds have been made with an NEP/A of 4.8×10^{-8} W cm^{-2} $Hz^{1/2}$. This time constant corresponds to a 10 to 90 percent rise time of about 4.2 msec. The NEP/A looks reasonable but the response time was too slow, the actual NEP were taken at 15 Hz, and noise spectra were not given. One could infer that by reconstructing these devices for a faster response, with some sacrifice in NEP one may be able to meet the NEP/A ratio. It would have to be demonstrated that the system would meet the required NEP/A for the complete required bandwidth and would give sufficient accuracies over the full dynamic range.

An estimate for an NEP/A for pyroelectric detectors can be made. From a manufacturer's data [3] a 2 x 2 mm^2 pyroelectric will exhibit at 350 Hz an NEP less than 2×10^{-9} W $Hz^{-1/2}$. This gives an NEP/A of 5×10^{-8} W cm^{-2} $Hz^{1/2}$. This is essentially the same NEP/A derived for the bolometer, but the noise data for the pyroelectric is clearly for the required operating frequencies, and the data incorporates a first stage of the detector electronics. As often supplied, the detector electronic package exhibits a 20 db per decade roll off in the responsivity with frequency. A compensating amplifier or a current feedback amplifier can be used to make the frequency response flat to well beyond 350 Hz. At the low frequency end these pyroelectrics will roll off because of a thermal time constant and a dc response is not possible.

From estimates of the current responsivity for pyroelectrics and noise factors for available amplifiers, it is possible to show that the range of increments in temperature of 7450:1 could be covered by a pyroelectric detector and a single current mode amplifier, but a full dynamic range of 7.5×10^5 is very unlikely.

The preceeding arguments have brought out a number of the difficulties of creating the detector arrays and they have not left us with any clear solution. Where the numbers come close there is little room for error in the assumptions and little room to allow for other potential problems that have not been mentioned. One cannot say that a thermocouple, thermistor or pyroelectric is best on theoretical grounds. One can compare specific devices with the data available. There still remain unknown factors such as the susceptibility to acoustic noise and EMI.

5.4 Suggested Solution

Because there do not exist commercially available systems to perform the tasks required, and because estimates based on available data do not leave much room for error, some prototype designs will have to be developed. Because a two-dimensional array has the potential for the widest dynamic range, it can fit into the required space and it can easily be synchronized with the laser pulses, this array of sensors which matches an area on the target board is suggested. Before developing the complete two-dimensional array, a single channel that can be duplicated later to 100 or more elements should be proven useful. The

proof should involve sensing the backside of a target plate upon which is incident laser pulses of the energy densities and repetition rate to be expected. A complete proof would involve operation within the drone environment with the drone in flight.

Three prototype designs can be pursued in parallel. One design assumes intimate contact with the target board and two designs read the radiated power from the surface. For the intimate contact design one could use thermocouples or themistors. For reading the radiated power, the designs could use thermocouples, thermistors, or pyroelectrics. In order to cover the complete dynamic range, the final system will probably require two of these designs, one for reading the absolute temperature to an accuracy of about 10 K and a second to read the differences in temperatures from pulse to pulse with a noise equivalent temperature of 0.004 K. The dual system would offer some crosscheck on the system operation and some redundancy in case of system failure. By using a dual system the dynamic range of each can be considerably smaller. The electronic bandwidths of the two systems can match the measurements better. The contacting system with a bandwidth of dc to 35 Hz could track up to 100 readings a second. A radiation monitoring system, responding to the transients in the temperature, with a bandwidth of 35 Hz to 350 Hz, will give a millisecond response.

With the development of the prototypes the design must account for the fact that they must be assembled in approximately a 100 element array. Compatibility of a dual system could also be in the design. It is possible that an array of off-the-shelf, one-inch diameter packaged pyroelectric-amplifier modules could operate as the transient temperature reading systems. There would then be room to feed contacting thermocouple wires between these modules to measure the absolute temperatures.

Again, it should be emphasized that the unknown factors of vibration and acoustic noises and EMI problems will have to be evaluated. It is recognized that pyroelectrics are also piezoelectric, but it is also true that sensitive thermocouples or bolometers with their associated electronics are "microphonic." There are schemes for mounting each of the devices to reduce the noise, and to what extent these will overcome the noise sources for this application will have to be determined experimentally.

5.5 References

[1] Most of the background information for the detector analysis can be found in "The Infrared Handbook," edited by W. L. Wolfe and G. J. Zissis, U.S. Government Printing Office (1978).

[2] E. H. Putley in "Optical and Infrared Detectors" edited by R. J. Keyes, Springer-Verlog, Berlin, Heidelberg, New York (1977).

[3] Lists of commercially available detectors are given in Laser Focus 1979 Buyers Guide, however, the data must be read with caution because the optimum value for one parameter may not occur at the same time as the optimum for another parameter.

[4] W. L. Block and Q. L. Gaddy, IEEE Journal of Quantum Electronics, QE-9, p 252 (1973).

6. Electronics Stage

6.1 Purpose

The purpose of this stage is to gather data from the detector array, store it, and subsequently transmit it to the ground station. The following constraints are assumed in the design of this stage. The electronics will be mounted inside a towed drone aircraft and, as a consequence, there will be strict limitations on size, weight, and power. Furthermore, the electronics must be airworthy if not flight certified. The drone will be towed at a speed of 130 to 150 m/s at a height of approximately 1 km (Above Ground Level). There will be no more than one experiment performed per pass over the ground station. Each experiment will consist of no more than 100 pulses. There will be no more than five (5) data points per detector per pulse spaced on integer multiples of 1 ms which are synchronized with the leading edge of the pulse. The detectors will be placed in a regular 10-by-10 array behind the target board. In addition to the detector, there will be additional channels of data designed to give information on the quality of the measurement.

6.2 Problems

It is clearly mandatory that the electronics must be constructed and mounted in a manner that prevents its operation from being degraded by the environment of the drone. Procedures and techniques for protecting the electronics against the detrimental effects of vibration, shock, and temperature, should be employed. Vibration seems to be a minor problem but shock may be much more serious. The equipment does not need to operate within specs during the shocks of launch and recovery but it must survive this trauma without losing its calibration. Temperature will have an effect on the calibration of the analog electronics and the A-to-D converters and it would be ideal if the temperature could be maintained at a fixed value, but if this cannot be done, the electronics' temperature should be measured as part of the experimental data.

There is ample power provided in the drone to run the electronics but converters will have to be incorporated to provide the specific voltages required by the electronics. Measurements of the power supply voltages and a calibrated, battery driven, source should be included in the data of each experiment.

Electromagnetic interference generated by the pulses with plasma ignition could be a problem but it should be possible to adequately shield the electronics from this influence. To avoid the possibility of EMI causing errors in the data transmission, the data for an entire experiment will be stored on board and transmitted down after the conclusion of the experiment.

The design of the signal conditioning and A-to-D conversion electronics must ameliorate the effects of a variety of error sources. The ones considered here are: quantization error, skew error, and aperture error. Quantization error comes from the fact that the A-to-D converter is attempting to represent a continous quantity with a limited number of discrete values. For a variety of reasons which will be explained later, we have chosen to

use an 8-bit converter. This implies that the full scale range is divided into 256 parts, and if the converter is working perfectly, gives an average worst-case error of ±0.2 percent of full scale. It is desired to achieve an accuracy of at least 10 percent of reading, and with the 8-bit converter, we will get a useful range of 25 to 1. As pointed out in the previous stage, this is insufficient to cover all situations and further discussion on how to accommodate this will be presented later. Skew error can occur when all of the elements of the detector matrix are not sampled at the same instant in time. If the time difference is significant, it will cause a distortion of the profile which is difficult to remove with subsequent data processing. For this reason as well as the ones mentioned in previous stages, a video type scan was eliminated from consideration as a viable technique. Aperture error is caused by the fact that uncertainty in the time that a sample was actually taken is reflected in a voltage uncertainty in the reading of an A-to-D converter. Designers generally try to keep the worst case aperture error about the same as the total quantization error. In this case, if the detector time constant is 1 ms and we use an 8-bit converter, the maximum allowable aperture is 3.9 μs. This implies that either the conversion time is less than 3.9 μs, or a sample-and-hold is used ahead of the converter.

It was pointed out earlier the range required to cover just the increments in emitted power from the target is estimated to be 745 to 1. To cover this range with one gain setting and with an accuracy of at least 10 percent of reading, we would require a 13-bit A-to-D converter. Using a converter of this size is not desirable because at the current state-of-the-art, it would be too slow, too expensive, and would necessitate increasing the memory size by 60 percent. The 8-bit converter will probably handle the dynamic range encountered in any given experiment. The difference between experiments can be handled by using sets of plug-in attenuators. To further enhance the available dynamic range, a delta coding scheme will be used, i.e., for any given detector, the current data point is the difference between the current output voltage and the output voltage which existed at the time the previous data point was taken.

The 8-bit converter was chosen because it seemed to be a good engineering compromise covering the following considerations: 8-bits will probably provide sufficient dynamic range for any given experiment; there is a good selection of single chip integrated circuits available which can perform the 8-bit converter function, inexpensively and with good speed; and it limits the memory to a reasonable size. In order to digitize the outputs of 100 detectors in 1 ms, a single analog multiplexer and A-to-D converter would have to be able to select and digitize any channel in 10 μs or less. This kind of performance requires rather sophisticated and expensive technology.

The memory is intended to store all of the data from one experiment so that it can be telemetered to the ground immediately following the experiment. The memory required can be calculated as follows: memory = 100 pulses x 5 samples/pulse/detector x 100 detectors x 1 byte/sample = 50,000 bytes. To this figure, additional memory would be added to store data designed to give information on the quality of the measurement. However, this does not represent an unreasonable amount of memory. It could be easily accomplished with either solid state memory chips or bubble memory. Bubble memory would be more compact but either could fit in the confines of the drone.

Data reduction aboard the drone was considered and rejected. The main motivation for doing data reduction on board would be to compact the data to reduce the bandwidth required for transmission to the ground. There does not seem to be an unreasonable amount of data in this case and furthermore, some methods of compaction destroy some aspect of the information contained in the data. Since this is an experimental endeavor, it would be best not to destroy any potential information.

The bit rate required to telemeter all of the data in 1 sec is about 0.5 Mbits/sec including some allowance for data framing and error checking. This rate is well within the capabilities of available technology, therefore, should not represent any problem in the design.

6.3 Suggested Solution

The above analysis points rather clearly to the design that should be used, with only a few choices to be resolved, consequently, the design should be straightforward and well within the available technology.

The design and construction of a scientific data logger should be done in a manner that future expansion can be easily accommodated. This suggests the use of standard circuit cards which are supplied by a variety of vendors. An example would be cards which support the "multibus" or the "std bus." Some of the cards could be standard products while the others would require special design.

While it is certainly possible to use a single A-to-D converter with a 100 channel multiplexer to scan the detectors, it appears that a more "solid" engineering choice would be to use one A-to-D converter per channel. It is possible to buy 8-bit, A-to-D converters for less than $10 each, making this approach cost only slightly more than a single converter but requiring much less performance. Each of the 100 detector channels would require two sample and hold circuits, one difference amplifier, and one 8-bit A-to-D converter. One sample and hold would be connected to the output of the detector amplifier, the other sample and hold would be connected to the output of the first, the inputs of the difference amplifier connected to the sample and hold outputs, and the A-to-D converter connected to the output of the difference amplifier.* The first sample and hold is triggered at the instant the detector output is to be sampled. After a small delay, the A-to-D converter is triggered. When the conversion is complete, the second sample and hold is triggered so that it saves the current detector voltage until the next sample. In this way, the A-to-D converter output will represent the voltage difference between the current detector output and the previous sample. All 100 detector channels would be doing the same thing at the same time

---

* This design assumes each voltage measurement is proportional to the temperature measurement rather than to the time derivative of the temperature. The design will have to be modified if the time derivative proves to be the better method.

so there would be no skew error. Each pulse would have five samples, the first would be triggered by an infrared detector placed to view a side lobe of the laser beam, the subsequent samples would be equally spaced from the first one by intervals which would be integer multiples of 1 ms. A ROM which plugs into the control portion of the electronics would determine the spacing for a particular experiment.

The output of the A-to-D converters are connected to a digital multiplexer which sequentially stores the converter output values into the memory. This multiplexer functions like a direct memory access channel (DMA) in that it supplies to the memory not only the data, but also the address where it is to be stored. This DMA is started when the conversion cycle is complete and ends when all of the data has been stored; there should be no problem completing this function before the next conversion cycle begins. The control electronics loads the starting address of the next detector scan in the DMA before the next scan begins.

The memory will be organized in standard computer fashion and will employ solid-state technology. Solid state is chosen over bubble memory because at this time it is a more mature technology and it is possible to get standard products which have 64 kbytes on a single board.

The control electronics would be implemented by a standard microprocessor board. This approach allows considerable flexibility in the details of how the data logging system should operate and does not require a special hardware design. The microprocessor could also format the data and add error checks in preparation for telemetering.

Since the data rates are in the vicinity of 0.5 MHz, it will be possible to use standard transmitters and receivers in the VHF band. If the data transmission requires one second, the drone will subtend an arc of about 8.5 degrees at the ground. This should pose no problem with the line-of-sight requirements for telemetry.

7. Special Measurements and Controls at the Drone

Special information is necessary when the drone flys past the laser system. This section discusses briefly the determination of this information. This section deviates from the basic format. Here we define a purpose and then discuss in sequence each of the special measurements and controls.

7.1 Purpose of this Stage

There are at least 16 special groups of measurements and controls that need to be made along with the beam-profile measurements. Others may occur as the target board is constructed. The known 16 are given below:

1. A pair of detectors get a timing pulse which shows when the laser pulse arrives at the drone. It also helps to detect air breakdown.
2. The absorption level measurements of the SF_6 and SiF_4 show the level of attenuation at various positions in the boundary layer.

3. The checks on the surface of the interface plate show where and when plasma ignition occurs.
4. The temperature limit check on the interface plate shows whether or not it stayed within the accepted range.
5. The position detectors show the angular orientation of the drone relative to the laser beam on a pulse-by-pulse basis.
6. The air flow rate shows a critical detail of the turbulence layer.
7. The rate of gas flow for the SF_6 and SiF_4 shows the expected attenuation level given (6).
8. The command signal #1 shows when to transmit the memory data.
9. The command signal #2 shows when to retransmit the memory data.
10. The command signal #3 shows the memory on the drone is full.
11. The command signal #4 causes a reset of the drone to the beginning of the data-taking sequence.
12. The command signals #5 to #20 are reserved for other communications, such as dc power level tests.
13. The green ready light on top of the drone shows that the drone is operating properly according to the measurement plan stored in the internal controller (microprocessor).
14. The flashing strobe light shows that something is wrong and that no further laser pulses should be sent.
15. A shock gauge for launch and crash conditions.
16. A control for opening and closing the sliding door.

We now discuss each of the above elements. Many require little discussion at this time since their purpose is obvious.

7.2 The Time Pulse

To allow maximum flexibility in the design of this target board, we assume that the laser pulse sequence is unknown. This assumption means we make our measurements of beam profile on a pulse by pulse basis. Because the interface plate causes a delay of about 10-100 μs before significant heat is seen, we use a start of the laser pulse with a signal from a pair of very fast detectors within a few microseconds to the array of detectors to make a measurement of the required baselines of each signal seen by each detector. We use two detectors placed so that they will see a side lobe of the laser beam at an irradiance level well below damage. These detectors are spaced so the interference minimum in the side lobes cannot be simultaneously seen by both detectors. The signal from these detectors are added together to produce the necessary signal for timing information. These detectors will have to be located where there is no SF_6. There are at least two possibilities: (a) put the detectors before ejected SF_6, or (b) put an aerodynamic pipe pointing toward the HEL laser system after the target board with a length that exceeds the turbulent boundary layer. Mount the detectors on a cross piece on this pipe so that they can see the reflected and diffused HEL beam. Air breakdown will be detected by measuring the fluence in the detectors and comparing that fluence with the peak fluence in the target board.

7.3 The Absorption Measurements

Here we use a small pulsed CO_2 laser (TEA range finder?) working at 10.6 μm or filtered to 10.6 μm and mounted within the drone. This calibrated beam is directed in a pipe with the necessary aerodynamics to a beam diverging mirror that causes the pulse to irradiate the active region around the interface plate at an angle of about 45 degrees for the center of that active region. To make the absorption measurements, two lines of detectors are placed so that they see the diverging mirror and do not see the HEL beam. Holes before and after the interface plate allow these detectors to see the prisms behind the holes which allow the calibrated beam to reach the detectors and which deflect the HEL beam away from these detectors to energy dumps. We suggest that there be at least three detectors in each line, one detector in the center and two at the edges of the active surface for the interface plate. In this way we can infer the surface of absorption.

The absorption measurements would be done by ratioing the measured energy per calibrated pulse out of the range finder with the measured energy per received pulse in each of the six detectors. This data would be adjusted with various geometry corrections, by assumptions about the distribution of the SF_6 and SiF_4 by measurements of the air flow, and by the measurements of the SF_6 and SiF_4 flow. The calibration pulses will be interleaved as necessary with the HEL pulses. The electronics of this absorption measurement system would select the evaluation of the energy in a pulse to the time windows of these received calibration pulses. A beam splitter at the range finder with a calibrated detector would be used to measure the energy per pulse before it goes through the pipe and the diverging mirror. To calibrate the geometry, the same system of detectors are used with a pure SiF_4 gas flow or without any SF_6 gas flow under the various air flow conditions. Since the angle effects can produce an increase of absorption length relative to that expected for the HEL beam by approximately a factor of two, we can expect the attenuation level to be around two orders of magnitude rather than the desired single order of magnitude.

7.4 Plasma Ignition Check

Because plasma ignition causes such catastrophic changes in measurement of beam profile, it is necessary to confirm that it has not occurred. The method of confirmation has to measure infrared radiation. To use detectors sensitive to visible radiation only will miss plasmas radiating only in the infrared. One possible configuration would be to use the same kind of 10.6 μm laser beam used to measure the SF_6 attenuation and cause this beam to pass over the active surface of the interface plate. By active measurement of the change in signal strength at any time during the application of an HEL beam and for several milliseconds afterward, there can be a positive monitor of the existence of plasma in front of the interface plate. A second configuration would be to have detectors that can see a change in the background radiation around 9.6 μm or some other selected band of wavelengths. This latter technique has the advantage that no active sources are necessary. The air acts as the frequency converter of the 10.6 μm radiation to the 9.6 μm radiation. The number of detectors needed for this process is determined by the field of view of each detector and

the places where these detectors can be located. A suggested placement is three-in-a-row parallel to the air stream above the active area of the interface plate and three-in-a-row also parallel with the air stream below the active area. All six detectors will have to be shielded from the HEL pulses and will have to be placed so that the air stream is not disturbed.

This discussion assumes that this measurement is used only to confirm that no plasma was ignited on the surface. It is not used to correct the beam profile if a plasma is ignited. In this case, a different configuration will be necessary and may not even be possible.

7.5 The Heat Limit Check

The purpose of this measurement is to confirm that the interface plate has no location that gets above the 400°C. The suggested approach for such a test is to use a fusable wire strung* between the detector array in appropriate contact with the back of the interface plate and set for a temperature of about 300°C. If a local hot spot develops, the wire will melt and a signal will result from the open circuit. The wire would be part of a bridge circuit.

7.6 Orientation of the Drone in Space

Four position detector arrays are placed at locations where the side-band pattern of the HEL beam will strike and where the SF_6 will not attenuate the beam. In front of each array are four pinholes that cause the laser beam to be defracted into interfering Airy disks. The cross defined by this pattern provides means to measure the orientation angles of the drone relative to the HEL beam. This information is necessary for accurate attenuation measurements and for correcting beam parameters. A single pinhole in conjunction with heliopots may prove to be the easier system to fabricate and use in this setup.

7.7 Air Flow Measurement

This measurement is necessary to deduce what is happening in the boundary layer. It is presumed that this measurement will be done between the laser pulses.

7.8 Gas Flow Rates of SF_6 and SiF_4 Mixture

This measurement is needed to correlate the attenuation to the actual rate of injection of this gas mixture. Associated with this measurement will be valves that control the rate of gas flow. There will be signals from the position of these valves. The simplest signal would be an on-and-off signal showing if a valve is entirely open. We suggest that this technique be used and that the gas flow out of the pressurized bottle have different sized orifices to control the gas flow.

---

* The local temperature of the plate will be higher than the local temperature of the wire because the contact point will have a temperature drop.

7.9 Command Signals for Control from #1 to #20

These signals are obvious and need only to be considered in the design.

7.10 The Signal Lights

It is very desirable to have on the drone two simple signals that everyone can see regardless of where they are. These signals could be radio or acoustic pulses if it turns out that people cannot look at the drone.

7.11 Shock Gauge

Here we need measurements of the shock and vibration (acoustic) level of the drone, at launch, during the flight, and finally at crash. In this way we can be sure the design limits have not been exceeded. If they are, then measures can be taken to modify the mounts so the shock, etc., is not critical.

7.12 Sliding Door

Because the drone will drop by parachute after each run, it is necessary to cover the target board so that (1) dust does not reach it and (2) there is a minimum chance of scratching it.

8. Software and Check List Issues

This section just lists possible necessary software, check lists, and numerical analysis that has to be developed once the actual target board is defined. It is premature to anticipate the detailed form of these efforts. We have chosen to delay these decisions by using a modular construction of the target board so that the final system is as flexible as possible to the variable conditions of the HEL tests.

8.1 The List of Needed Numerical Analysis

1. A model showing the time response of the heat pulse.*
2. A model showing the analog signal through the electronics with noise.
3. A model showing the digital conversion process of the signal to storage into the memory with noise.
4. A model showing the coding for two levels of error detection with noise.
5. A model showing the transmission and reception process.
6. A model showing the conversion of the received digital data stream.
7. A model showing the attenuation process with accuracies.
8. A model showing the expected beam profile structure.
9. A model showing the precedures for computing desired beam parameters from the expected structure. (Suggest using the cubic spline approach.)

---

* Repeating pulses imply a complex coupling of heat between laser pulses. This has to be analyzed using something like the cubic spline approach.

10. A model showing the influence of the plasma on the beam profile structure.
11. A model showing the influence of the SF_6 on the beam profile.
12. A model showing how the propagation process changes the beam profile.
13. A model showing how the pointing and tracking process changes the beam profile.

8.2 The List of Computer Programs

1. The microprocessor programs used for controlling the sequence of data acquisition in the drone during a measurement run. Expect different programs for each site.
2. The minicomputer programs used at the fixed site for calibration work and for reducing the received data from the drone into the desired beam parameters on a pulse-by-pulse basis.
3. Various graphics programs to present the data of the beam parameters for the data within a measurement run and between measurement runs of the drone.
4. Various statistics programs to compute the statistics for the beam parameters from all runs, selected runs, and selected pulses.
5. Contour plots of the raw data on a pulse-by-pulse basis.
6. Programs for residual contour plots of the beam profile showing the errors between the inferred beam profile and the raw measurements.
7. Data storage programs of raw data so that appropriate mathematical models can be developed to allow minimum storage of information and to select the proper features in the evaluation of the interaction process between the target board and the HEL pulse train.
8. Check lists stored in the computer which will be used to make sure measurement runs are being done properly and consistently.

8.3 The Check Lists

During a run of measurements, it will prove useful to develop check lists so that necessary equipment is turned on in the proper sequence and so that data is developed as needed and is reliable. Examples are:

1. Develop data handling logs and notebooks that would be systematically updated as work progresses,
2. Calibration check lists at the fixed site,
3. Drone handling check lists before flight,
4. Drone handling check lists after flight,
5. Drone handling check lists during flight,
6. Receiver check lists for data storage and use,
7. Computer handling check lists, and
8. Check-out procedures for the individual equipment during the development stages of the target board so they can be duplicated if necessary. Include the manufacturers, other sources, and the purchasing forms.

9. Calibration Issues

This section just lists the various critical elements in calibration strategy that will be needed as the target board is used in measurements.

1. Because the target board system is complex, it will be necessary to check the entire system including the interface board and the received data at the computer on the ground. One technique may be to use a calibrated heat lamp assembly that would be mounted on the drone when it is not flying and to cause an entire heating sequence up to the 400°C to be applied to the target board before a measurement run. Then transmit the measured and stored data both before and after the drone is in the air to the ground receiver and computer system for recording and computing the implied results.
2. It is very desirable to develop key checks and control charts of these key checks so that history of various parts of the target board system is easily seen. In this way we have a visual and consistent history of the various parts of this measurement system.
3. Finally, whatever technique is used to test and to calibrate parts of this system, they should be used consistently throughout the entire history of the target board system. This is the only way to be sure the data is consistent over this time period. We can expect numerous parts of this target board system to change because it will be subject to a harsh environment.

10. Conclusions

10.1 Summary of Suggested Solutions

1. Make sure the peak irradiance is always less than 5 MW/cm^2 to avoid dirty air breakdown. A test without drone or other equipment could provide the beam propagation conditions at each site. If safety precludes open air propagation, then use a simple target board for such tests such as an aluminum sheet that has been polished and is curved for diverging the reflected beam into the ground.
2. Test if the SF_6 can be made a calibrated attenuator for the absorption range of 0 to 90 percent. (See 9.)
3. Construct the two microscopically smooth copper sheets that are treated to avoid prompt ignition.
4. Test the number of temperature cycles from 100°C to 400°C the above plates can take and still maintain the desired smoothness. (See 11.)
5. Test the plasma ignition threshold for the above units with and without the SF_6 at selected times in the above test (4). For example, every tenth cycle would give sufficient data assuming the plate is stable for at least a hundred cycles.
6. Test if the NaCl wedge can be the beam splitter for the calibration of the target board and its electronics.
7. Construct three units using a detector, the A/D unit, and memory. These units would test acoustic noise, shock, and other environmental hazards in the drone. Use one unit

with a pyroelectric detector, a second with a thin film detector, and a third using contacting thermocouples. After these tests, decide which is the appropriate system under the conditions for the drone flight.

8. Go ahead with the design of the electronics assembly including the sample-and-hold circuits, the A/D conversion, the memory, and the telemetry unit. This system is insensitive to the problems associated with the detector-preamplifier unit and with the target board. There could be some problems due to shock in the landing of the drone. This step implies a decision to have no mini-calorimeters as the detectors.
9. Make test setups with the drone to see if the SF_6 scheme can be used. Do this effort without the laser system and the expensive target board.
10. Get constructed a number of polished and unpolished plates for the target board which are made of Al and stainless steel. These will be used as test plates during various shakedown runs.
11. Develop a means for confirming the change in the integrated scatter from the surface of the target plate using a scanning 10.6 μm laser beam. This setup will probably have to be in a laboratory.
12. Decide whether plasma ignition will have to be accepted in the measurement process, given the above test results.
13. Decide if the target board can or needs to be machined to show thermal mode behavior.
14. Decide on the proper detector and preamplifier for the drone system. Note the issues in sections 4, 5, and 6 relative to appropriate data sampling during a heat pulse. Of particular importance in this issue is an answer to the question: What type of radiation measurement should be performed given the previous test results and the nonlinearity of the heat flow around and in the target board.
15. Select and construct the mathematical models and computer programs so that they are ready as the equipment becomes ready.
16. Assemble the equipment for the fixed site.
17. Develop the calibration strategies at the fixed site given the results from above tests and the new data about the actual laser system that will be available at this time.
18. Avoid water vapor on all optical surfaces such as the copper-gold plate, the anodized aluminum plates, and the NaCl wedge.

10.2 Direct Answers to the Questions Posed in Appendix A

1. The fluence in excess of 1 J/cm^2 and irradiance in excess of 1 MW/cm^2 may cause plasma ignition. As a consequence, special effort is necessary to avoid plasma ignition. Current state-of-the-art measurement techniques used with cw lasers fail to account for this potentiality. Therefore, use of these techniques without modification would require a restriction of either the applied fluence to be below 1 J/cm^2 or the applied irradiance to be below 1 MW/cm^2 to avoid plasma ignition. This severe restriction is inconsistent with the desired fluences and irradiances. (See the discussion in question (3) for a potential use of the current target board.)

2. A metal plate with an array of holes may work if the microscopic smoothness on the edges of the holes can be constructed so that there is little chance for creating metal or oxide flakes. Since normal drilling and surface working techniques do not deal with these demands for microscopic smoothness, it is necessary to perform special efforts to get such a plate that will raise the threshold for plasma ignition. Our conclusion is to avoid this approach for either the fixed site or the drone. Instead we suggest a polished copper plate with gold plating and no holes be used as the target board. We expect a fluence of 10 to 20 J/cm^2 without plasma ignition.

   The dielectric slab of NaCl or KCl apparently can take the design fluence of 120 J/cm^2. However, they are hygroscopic and require a very clean environment to keep their surface clean of water and dirt. This need for cleanliness is possible for the fixed site and is questionable for the drone. A single landing of the drone will probably cause significant dust and shock problems.

3. Because the target board is subject to damage and change, it is desirable to use radiometry type techniques to observe the radiative temperature from the back of the target board. This means the detectors have a minimum level of sensitivity. The pyroelectric detector has the greatest sensitivity relative to signal-to-noise and therefore is best compared to the thin film and the thermocouple detectors. Unfortunately, the pyroelectric is sensitive to acoustic noise and will require special mounting to minimize those effects. If these conditions can be satisfied, then the pyroelectric is a good choice. If there is a failure, then the necessary strategy is to accept a smaller dynamic range for the temperature rises. For example, we could set the radiative temperature rise from 1°K to 50°K instead of the 0.04°K to 5°K range so that the thin film detectors can work accurately with the necessary time response and signal to noise. If we need to measure a lower temperature level, we change the target board from copper to either stainless steel or anodized aluminum so that the temperature rise of the heat pulses are within the optimum range of the thin film detectors. We have a factor of 3 increase in temperature rise using stainless steel and 47 times increase in temperature rise using anodized Al.

   It may prove possible to use the current electronics, thin film detector, and telemetry set up currently under development for cw laser sources. The hole plate of this unit would be changed to the gold-plated copper sheet with no holes. We need to test the range within which the current drone system can act as a radiometer with the desired accuracy of 10 percent. The sampling strategies of the current target board will have to be validated as relevant to radiometry measurements.

   There is a key issue on the form of the voltage measurements. The pyroelectric is sensitive to the derivative of the temperature, while the thin film is sensitive to the temperature. Given the nonlinearity in the temperature response, the thin film may prove to be the better method because it directly relates to the temperature.

   In conclusion, the selection of the proper detector is open at this time. This situation is why we suggest the construction of the three-detector A/D converter, etc., channels.

4. Section 6 discusses the data handling techniques. In brief, there is minimum preprocessing of the measured data because there are significant calibration corrections and uncertainties in the actual choice of models for reducing the measured data. The needed speed for transmission after a series of laser pulses is such that radio frequencies are sufficient. Unlike the laser transmitter, the beam width of the radio signal is broad, therefore, the receiver need not have complex tracking capabilities. We have rejected optical processing as not feasible for the drone or the fixed site. Optical fibers are also not useful at this time in either the drone or the fixed site. It may prove useful to have optical fibers for the communication between the front payload and the back payload of the drone. At present, that question cannot be answered. The transmission of data anywhere should be via pulse-coded-error-checking signals. Bulk data transmission will be from the drone to the receiver at the fixed site. A minicomputer there will convert the bulk data into desired forms for presentation to the operator of the laser. Command signals will be sent to and received from the fixed site from the laser unit. The transmitter at the fixed site will relay the command signals from either the drone to the laser or vice versa via a radio signal. The visual signal on the drone will provide the fail safe test for a valid measurement run. A microprocessor will define a command sequence during a measurement run. This computer will be preprogrammed and on board the drone.

The present plan is to send data only before and after a measurement run. The transmission and measurement system would have to be reconsidered if it becomes desirable for direct communications on a pulse-by-pulse basis. That system would be very expensive.

11. Acknowledgments

There are many persons who have contributed freely of their valuable time to help us make the judgments on the measurement situation. Because they are numerous, we just indicate the various institutions, namely AFWL, NRL, MIRADCOM, Battelle, AVCO, PSI, RRI, NWC, AFMC, and NBS.

The key idea for the potential use of SF_6 in front of the target plate arose from a series of conversations with Lt. Col. R. Grotbeck, C. T. Walters, R. Rudders, and R. Root.

The library services of NOAA, DoD, and RRI were very helpful in extracting the needed data from the technical literature, both unclassified and classified.

APPENDIX A

1. Current target board technology employs thin-film bolometers to sample the far-field pattern produced by continuous-wave infrared lasers. We have a requirement to build and operate a target board capable of sampling ir laser pulses of approximately 10 μs duration.
2. Far-field parameters of interest are the peak fluence (J/cm^2), the coordinates of this peak, the area of the fluence contour at e^{-2} of the peak fluence, and the coordinates of the centroid of the fluence in this area. To obtain reliable and reproducible measurements of these parameters, several important questions must be answered. (1) What methods within the current state-of-the-art allow proper attenuation and sampling of the pulsed beam? (2) Will a metal plate with an array of holes or a dielectric slab work? (3) What type of detectors currently available will function properly under the environmental conditions prevailing at outdoor target sites (pyroelectrics, thin-film bolometers, other)? (4) What data handling techniques are appropriate to relay information from outdoor target sites to the operator of the pulsed laser? For example, microprocessing, optical processing, optical fibers, radio or laser telemetry.
3. We request that NBS gather information to answer the questions proposed above. The performance period of this project will run from June 1979 to September 1979. The project will culminate in a single comprehensive report within one month after the performance period. This report will summarize all information gathered and suggest a course of action resulting in the production of a pulsed laser target board. Constraints, compromises, and viable alternatives to the suggested approach will also be noted in the report.

NBS-114A (REV. 9-78)

U.S. DEPT. OF COMM. BIBLIOGRAPHIC DATA SHEET	1. PUBLICATION OR REPORT NO. NBSIR 80-1628	2. Gov't. Accession No.	3. Recipient's Accession No.

4. TITLE AND SUBTITLE

Measuring Features of the Fluence at the Far Field of A CO_2 Pulsed Laser - An Issue Study with Suggestions on How to Do It

5. Publication Date

April 1980

6. Performing Organization Code

7. AUTHOR(S)

Eric G. Johnson, Jr., Robert J. Phelan, Jr. & Don R. Boyle

8. Performing Organ. Report No.

9. PERFORMING ORGANIZATION NAME AND ADDRESS

NATIONAL BUREAU OF STANDARDS
DEPARTMENT OF COMMERCE
WASHINGTON, DC 20234

10. Project/Task/Work Unit No.

11. Contract/Grant No.

12. SPONSORING ORGANIZATION NAME AND COMPLETE ADDRESS *(Street, City, State, ZIP)*

Same as Block #9

13. Type of Report & Period Covered

14. Sponsoring Agency Code

15. SUPPLEMENTARY NOTES

☐ Document describes a computer program; SF-185, FIPS Software Summary, is attached.

16. ABSTRACT *(A 200-word or less factual summary of most significant information. If document includes a significant bibliography or literature survey, mention it here.)*

This study examines the problems for measuring the energy density incident on targets where the energy is from a pulse of high energy at CO_2 wavelengths and where the targets are located at the far field. The analysis considers two targets--first, a ground-based target for testing and calibration of the measurement systems and second, a drone towed behind an airplane from which the energy distribution information is telemetered to the ground station. Although certain design limits are assumed, the results are general and therefore specific data about the laser sources is not supplied.

This study traces each stage of the measurement system from the reception of the incident laser pulse on the drone to the pulse-coded transmission of the sampled data to a ground-based computer.

The basic conclusion is that not all desired conditions of potential fluence can be studied. Plasma effects can prevent proper measurements. If the suggested SF_6 gas can act as a calibrated attenuator and hence avoid the plasma effects, then the range of potential fluences can be increased substantially.

17. KEY WORDS *(six to twelve entries; alphabetical order; capitalize only the first letter of the first key word unless a proper name; separated by semicolons)*

Attenuators; beam profile; calorimetry; fluence; irradiance; heat flow; measurements of temperature; plasma effects; pulsed laser beams; 10.6 μm.

18. AVAILABILITY ☒ Unlimited

☐ For Official Distribution. Do Not Release to NTIS

☐ Order From Sup. of Doc., U.S. Government Printing Office, Washington, DC 20402, SD Stock No. SN003-003-

☒ Order From National Technical Information Service (NTIS), Springfield, VA. 22161

19. SECURITY CLASS (THIS REPORT)	21. NO. OF PRINTED PAGES
UNCLASSIFIED	56
20. SECURITY CLASS (THIS PAGE)	**22. Price**
UNCLASSIFIED	$7.00

USCOMM-DC